Journal of Medicinal Chemistry

Article

pubs.acs.org/jmc

Synthesis of Novel Tricyclic Chromenone-Based Inhibitors of IRE-1 RNase Activity

Sujeewa Ranatunga,[†] Chih-Hang Anthony Tang,[‡] Chang Won Kang,[†] Crystina L. Kriss,[‡] Bernhard J. Kloppenburg,[†,‡] Chih-Chi Andrew Hu,*[,‡] and Juan R. Del Valle*[,†]

[†]Drug Discovery Department and [‡]Department of Immunology, H. Lee Moffitt Cancer Center and Research Institute, 12902 Magnolia Drive MRC3E, Tampa, Florida 33612, United States

Supporting Information

ABSTRACT: Inositol-requiring enzyme 1 (IRE-1) is a kinase/RNase ER stress sensor that is activated in response to excessive accumulation of unfolded proteins, hypoxic conditions, calcium imbalance, and other stress stimuli. Activation of IRE-1 RNase function exerts a cytoprotective effect and has been implicated in the progression of cancer via increased expression of the transcription factor XBP-1s. Here, we describe the synthesis and biological evaluation of novel chromenone-based covalent inhibitors of IRE-1. Preparation of a family of 8-formyltetrahydrochromeno[3,4-*c*]pyridines was achieved via a Duff formylation that is attended by an unusual cyclization reaction. Biological evaluation in vitro and in whole cells led to the identification of **30** as a potent inhibitor of IRE-1 RNase activity and XBP-1s expression in wild type B cells and human mantle cell lymphoma cell lines.

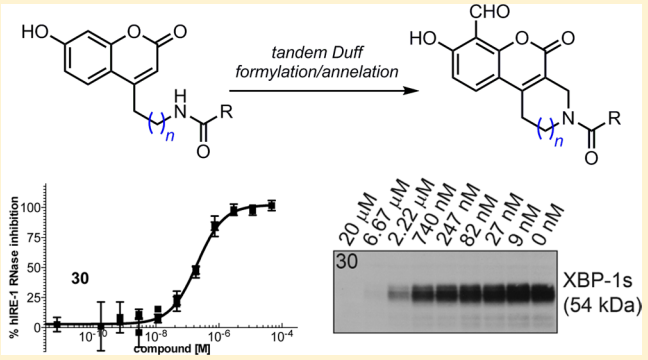

INTRODUCTION

The endoplasmic reticulum (ER) stress response is a cytoprotective mechanism activated in response to proteotoxic burden and is crucial for homeostatic regulation.[1,2] Disruption in the stoichiometric balance, transport, or processing of intracellular proteins leads to the activation of three distinct pathways mediated by the ER stress sensor proteins IRE-1, ATF6, and PERK. IRE-1 is unique in that it contains a stress sensor domain in the lumen of the ER and a cytosolic serine/threonine kinase domain linked to an RNase domain. Multiple stress conditions can cause IRE-1 to oligomerize. Oligomerization brings the IRE-1 cytoplasmic kinase domains into proximity, allowing for autophosphorylation and activation IRE-1 RNase activity. The IRE-1 RNase domain is critical for the function of IRE-1 because it splices 26 nucleotides from the mRNA of X-box binding protein 1 (XBP-1), causing a frame shift in translation.[3−5] The spliced XBP-1 mRNA encodes a functional 54 kDa XBP-1s protein in mammalian cells, which is a transcription factor that translocates into the nucleus and regulates ER stress response genes.

Since gene copy number amplifications and aberrant protein expression are hallmarks of cancer, many human tumors rely on a robust ER stress response for growth and survival.[6,7] As a result, IRE-1 and related stress sensors have emerged as potential therapeutic targets for the treatment of cancer.[8−10] IRE-1-mediated activation of XBP-1 has also been implicated in the evasion of virus-induced cytotoxicity[11] as well as in the development of inflammatory arthritis.[12,13] Small molecules capable of modulating IRE-1 RNase activity and XBP-1s transcription thus represent useful chemical tools and potential therapeutic agents.

Efforts to identify inhibitors of IRE-1 RNase function have relied primarily on high-throughput screening of large chemical libraries. This has led to the discovery of various salicylaldehydes with in vitro activity against IRE-1-mediated mRNA splicing.[14−17] A limited number of nonelectrophilic inhibitors of IRE-1 RNase activity have also been reported (Figure 1).[18,19] While aldehydes and related functional groups are generally considered undesirable with respect to chemical probe development, the recent FDA approval of various electrophilic drugs has renewed interest in covalent inhibitors.[20] The importance of the aldehyde moiety for potent IRE-1 RNase inhibition by **5** (4μ8C)[15] and related compounds has been rationalized by the formation of an unusually stable Schiff base with lysine 907 in the IRE-1 endonuclease domain.[21] Although IRE-1 contains 25 lysine residues in its cytosolic domain, only covalent modification at K907 (and in some cases K599) is observed in vivo.[15] This selectivity has been attributed to specific perturbation of the K907 ε-amino group pK_a, resulting in enhanced nucleophilicity, increased rate of Schiff base formation with aldehyde inhibitors, and slow off-rate.

Here, we report the synthesis and biological evaluation of novel chromenone-based inhibitors of IRE-1 RNase activity. A tandem Duff formylation/annelation reaction en route to candidate inhibtors gave rise to fused tricyclic chromenopiper-

Received: February 14, 2014
Published: April 21, 2014

   dx.doi.org/10.1021/jm5002452 | *J. Med. Chem.* 2014, 57, 4289−4301

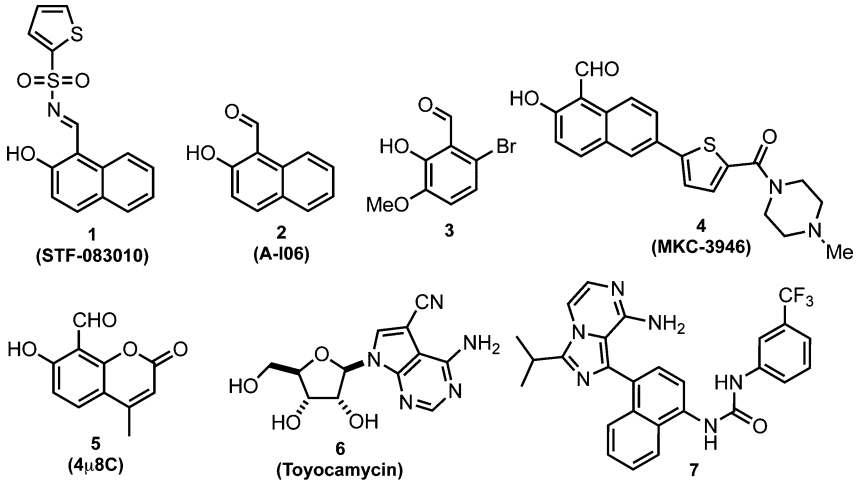

Figure 1. Selected known inhibitors of IRE-1 RNase activity.

idine, chromenoazepane, and chromenoazecane scaffolds. Selected analogues based on a tetrahydrochromeno[3,4-*c*]pyridine core structure potently inhibit XBP-1 splicing in vitro and block the expression of XBP-1s in whole cells, making them useful compounds for interrogating IRE-1 RNase activity in biological systems.

RESULTS AND DISCUSSION

FRET-Suppression Assay of Potential IRE-1 Inhibitors. To assess the in vitro activity of potential IRE-1 RNase inhibitors, we carried out the expression and purification of recombinant human IRE-1 for use in an in vitro FRET-suppression assay.[17] The cytoplasmic kinase/RNase domain (aa 547−977) of human IRE-1 was expressed as a soluble puritin-His-tagged 59 kDa fusion protein in SF21 cells and purified by Ni-NTA affinity chromatography. To confirm that hIRE-1 exhibited a functional RNase domain, we evaluated its activity in vitro using a synthetic mRNA stem-loop corresponding to the XBP-1 substrate sequence. This stem-loop incorporates a Cy5 fluorophore on its 5′ end and the black hole quencher (BHQ) on its 3′ end, resulting in fluorescence only upon site-specific cleavage by the protein. Protein (5 nM) was incubated in a 96-well plate at room temperature with different concentrations of the XPB-1 stem loop for up to 2 h, and fluorescence was measured upon excitation and emission at 620 and 680 nm, respectively. Recombinant hIRE-1 exhibited functional RNase activity wth a K_m value of 45 nM (see Supporting Information).

We first evaluated a small set of known IRE-1 inhibitors, synthetic analogues, and selected commercially available salicylaldehyde derivatives using the FRET-suppression assay (Figure 2). We recently reported the in vivo characterization of naphthaldehyde derivative **2** (A-I06), which was postulated to be the bioactive breakdown product of the known IRE-1 inhibitor **1** (STF-038010).[22] When evaluated in our assay, **1** and **2** exhibit similar IC_{50} values (9.94 and 9.73 μM, respectively), while decomposition product **8** and reduced derivative **9** showed no appreciable inhibition at 20 μM. Interestingly, the salicylaldehyde moiety alone was not sufficient for IRE-1 RNase inhibition, as evidenced by the weak activity (>20 μM IC_{50}) of compounds **10**−**13**. Modification of the aldehyde or phenol functionalities also resulted in inactive compounds (**14**−**16**). Coumarin derivative **5**, recently identified in a high-throughput screening effort,[15]

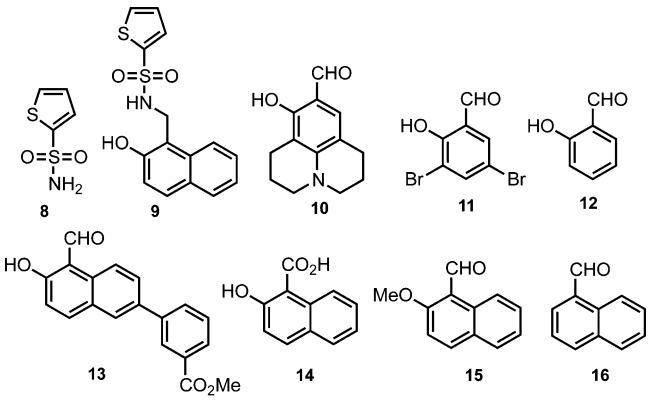

compound	IC_{50} (nM)	95% CI (nM)
1	9939	(3692 - 26760)
2	9732	(5057 - 18730)
5	206	(142 - 297)
8	>20000	-
9	>20000	-
10	>20000	-
11	>20000	-
12	>20000	-
13	>20000	-
14	>20000	-
15	>20000	-
16	>20000	-

Figure 2. Compounds evaluated for anti-IRE-1 RNase activity by FRET-suppression assay. IC_{50} and CI values are reported as the mean of four separate experiments.

exhibited significantly enhanced potency against IRE-1 RNase function with an IC_{50} value of 206 nM in our FRET-suppression assay.

Synthesis of Tricyclic Chromenones. In an effort toward functionalized derivatives of **5** for use in covalent tagging and pulldown experiments, we synthesized analogues **20a**−**d** in four steps from the appropriate amino acids (Figure 3). Installation of the aldehyde moiety in each case relied on a Duff formylation carried out using hexamethylenetetramine (HMTA) in refluxing glacial acetic acid. Interestingly, when the reaction was carried out in refluxing TFA using

dx.doi.org/10.1021/jm5002452 | J. Med. Chem. 2014, 57, 4289−4301

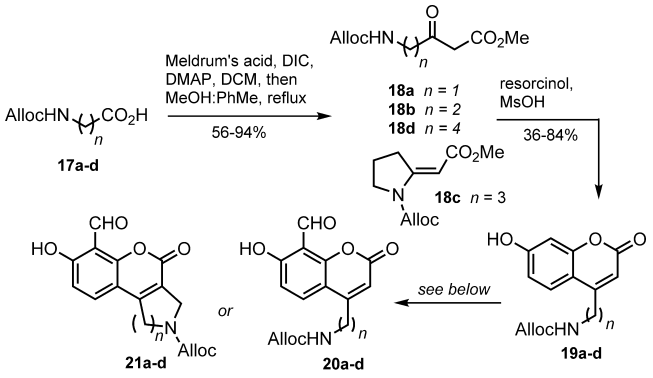

substrate	conditions[a]	product	% yield
19a	A	**20a**	4
19a	B	**20a**	4
19a	C	**20a**	4
19b	A	**20b**	10
19b	B	**21b**	22
19b	C	**21b**	41
19c	A	**20c**	13
19c	B	**21c**	18
19c	C	**21c**	17
19d	A	**20d**	15
19d	B	**21d**	3
19d	C	**21d**	9

[a]Reaction conditions: (A) 3 eq. HMTA, AcOH, 95-100 °C, 24h, (B) 3 eq. hexamine, TFA, 75 °C, 24h, (C) Ac_2O, pyridine, MeCN, then 3 eq. HMTA, TFA, 75 °C, 24h. All conditions were followed by acidic workup.

Figure 3. Synthesis of substituted bicyclic and tricyclic 8-formyl chromenones.

intermediate **19b** as a starting material, formylation was attended by an annelation involving the pendent carbamate nitrogen to give tetrahydrochromeno[3,4-*c*]pyridine **21b** as the sole product. The structure and connectivity of this tricyclic scaffold were confirmed by HMBC NMR. As is typically the case for Duff formylations,[23,24] complete consumption of **19** still resulted in low yields of **20** and **21** due to significant decomposition. However, the yield of **21b** improved to 41% when the reaction was preceded by acetylation of the *o*-hydroxyl group.

A plausible mechanism for the formation of **21b** involves electrophilic aromatic substitution at position 3 of the chromenone core (Scheme 1). The reaction of electron rich aromatics with HMTA in organic acid occasionally results in aminomethylation in addition to formylation via decomposition of intermediates such as **B**.[23,24] In the case of **21b**, this decomposition is likely precluded by attack of the carbamate nitrogen onto the electrophilic methylene group in **C**. The interrupted Duff reaction at position 3 presumably occurs prior to formylation at position 8, as the use of only 1 equiv of HMTA in refluxing TFA afforded intermediate **D** as the major product from **19b**. The concomitant annelation was not observed in the case of substrate **19a** under any of the conditions listed in Figure 2. However, hexahydrochromeno-[3,4-*c*]azepine **21c** and hexahydrochromeno[3,4-*c*]azocine **21d** were isolated as the sole products from **19c** and **19d** when TFA was used as the solvent.

Scheme 1. Proposed Mechanism of Cyclization during Duff Formylation

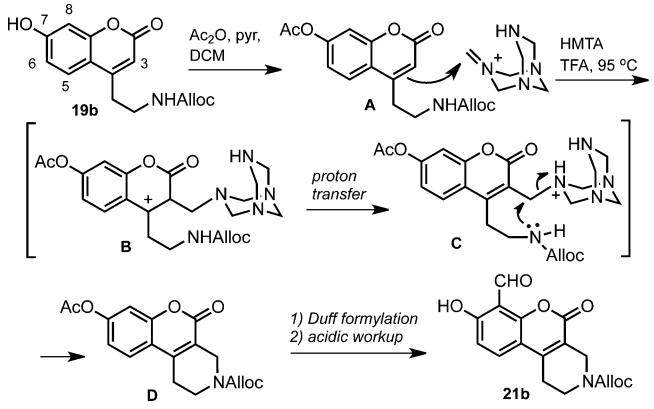

Structure–Activity Relationships. When evaluated in the FRET-suppression assay, bicyclic derivatives **19a–d** exhibited inhibitory activities in the 100–500 nM range (Figure 4). The

compound	IC_{50} (nM)	95% CI (nM)
5	206	(142 - 297)
20a	472	(229 - 971)
20b	296	(151 - 580)
20c	181	(156 - 210)
20d	118	(93 - 148)
21b	111	(76 - 162)
21c	118	(105 - 197)
21d	150	(126 - 178)

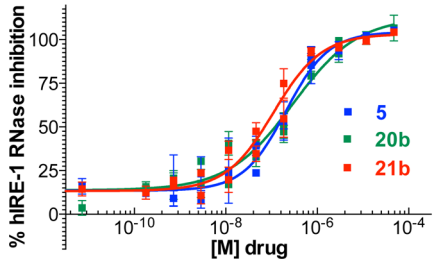

Figure 4. In vitro inhibition of IRE-1 RNase activity by compounds **20** and **21**. IC_{50} and CI values are reported as the mean of four separate experiments.

constrained tricyclic derivative **21b** consistently showed enhanced activity against IRE-1 RNase activity relative to the bicyclic compounds **20b** and **5** in side-by-side experiments. Given the optimal in vitro potency and chemical yield of **21b**, we carried out the synthesis of a family of analogues to assess the importance of the hydroxyl group and the distal N-substituent (Scheme 2). A potential covalent irreversible inhibitor **23** was obtained by chlorination of the reduced derivative **22**. Compounds **24** and **25** were prepared by acid-catalyzed protection of the aldehyde in **21b** as the 1,3-dioxane or dithiane derivative. Analogues **26** and **27** were prepared by O-alkylation of **24**, followed by acidic hydrolysis of the dioxane. Compounds **29–34** were synthesized by reaction of intermediate **28** with various acylating or alkylating reagents, followed by acidolysis.

The presumed importance of the aldehyde functionality for IRE-1 RNase inhibition also prompted us to explore alternative

dx.doi.org/10.1021/jm5002452 | J. Med. Chem. 2014, 57, 4289–4301

Scheme 2. Synthesis of O- and N-Substituted Analogues

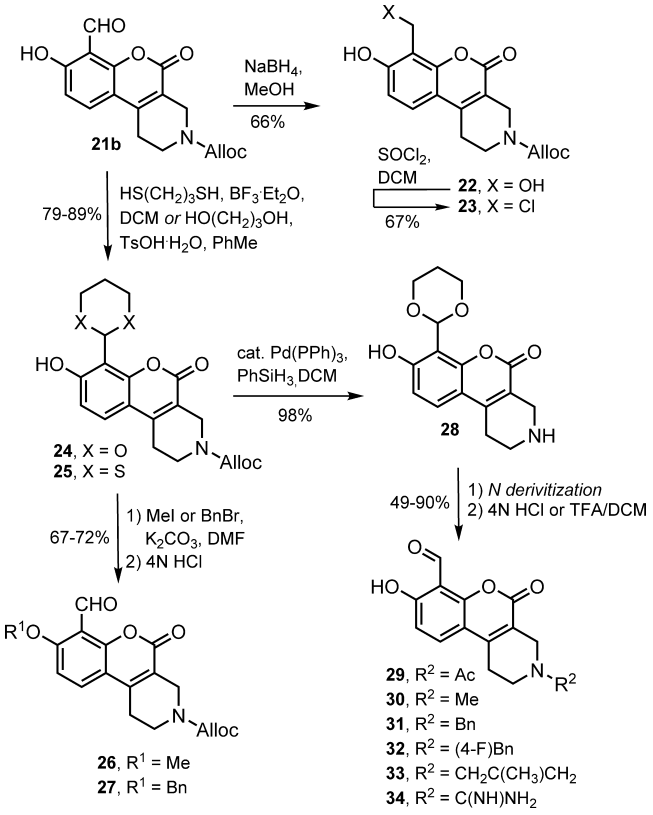

electrophilic groups at the 8 position of the chromenone core. Scheme 3 depicts the synthesis of analogues **36**–**42** from compound **21b**. Formation of the ketone in **36** via oxidation of the Grignard product required prior protection of the *o*-hydroxyl as methoxymethyl ether **35**. Olefination of **35** and acetal hydrolysis afforded electrophilic analogues **37** and **38**.

Scheme 3. Synthesis of Analogues with Aldehyde Surrogates

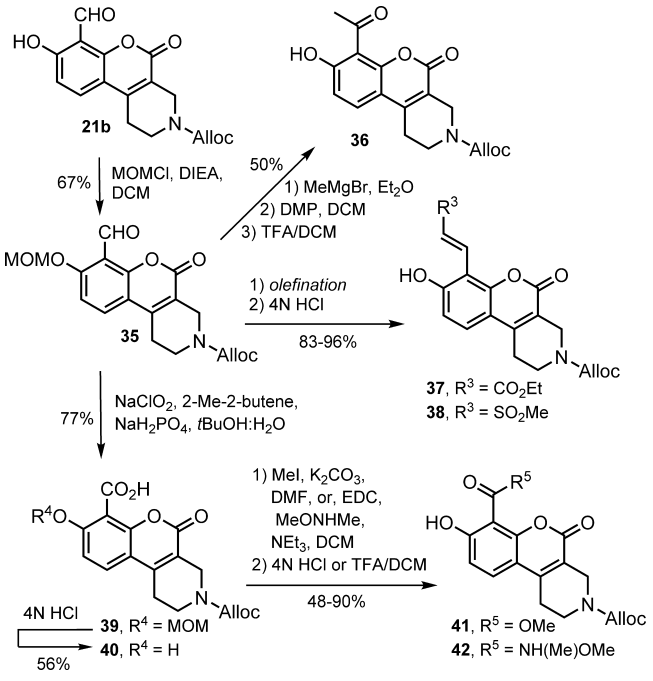

Oxidized variants **40**–**42** were synthesized via Pinnick oxidation of **35**.

All compounds were evaluated by FRET-suppression assay in side-by-side experiments using **21b** as a control inhibitor (Table 1). As anticipated, protection of the aldehyde group in

Table 1. In Vitro IRE-1 RNase Inhibition by Analogues of 21b

compd	IC_{50} (nM)	95% CI (nM)
21b	111	76–162
22	>20000	
23	>20000	
24	3051	2031–4584
25	16210	12900–20360
26	>20000	
27	>20000	
28	1230	704–2148
29	312	222–439
30	200	149–268
31	113	62–207
32	303	181–500
33	255	183–354
34	47	35–64
35	>20000	
36	>20000	
37	1718	1289–2288
38	>20000	
40	4109	3099–5448
41	5644	3902–8162
42	>20000	

21b as the 1,3-dioxane or dithiane acetal (**24** and **25**) resulted in weaker IRE-1 inhibitory activity. Alkylation of the phenol oxygen (compounds **26**, **27**, and **35**) resulted in a complete loss of potency below 20 μM. The *N*-acyl derivative **29** exhibited an IC_{50} value of 312 nM, while *N*-alkyl analogues **30**–**33** were found to be slightly more potent. Interestingly, *N*-benzyl analogue **31** was almost 3-fold more active than the corresponding fluorinated derivative **32**. Guanidinylation to give **34** resulted in a notable increase in potency (IC_{50} = 47 nM) relative to the parent compound, though solubility significantly decreased. Ketone **36**, vinyl sulfone **38**, and Weinreb amide **42** showed no significant IRE-1 RNase inhibitory activity below 20 μM. However, electrophilic compounds **37**, **40**, and **41** displayed moderate potency (1–5 μM) in vitro. Also of note, 1,3-dioxane derivative **24** exhibited an in vitro IC_{50} of 3.1 μM, whereas the corresponding 1,3-dithiane analogue **25** displayed more than 5-fold weaker activity. To confirm that the enhanced inhibitory activity of **24** is not simply a function of a labile aldehyde masking group, we carried out stability studies in assay buffer and observed no significant decomposition of the 1,3-dioxane moiety over 12 h (see Supporting Information).

Inhibition of XBP-1s Expression in Whole Cells. In order to determine whether our inhibitors could block the expression of XBP-1s in whole cells, we incubated LPS-stimulated B cells from the spleens of wild-type mice with 20 μM selected compounds for 24 h, lysed the cells, and analyzed the lysates for the expression of XBP-1s by immunoblots. Compounds **29** and **30** potently suppress the expression of XBP-1s at 20 μM in wild-type mouse B cells (Figure 5A). In addition, **5**, **21b**, and **24** exhibit strong inhibition of XBP-1s, as

dx.doi.org/10.1021/jm5002452 | J. Med. Chem. 2014, 57, 4289–4301

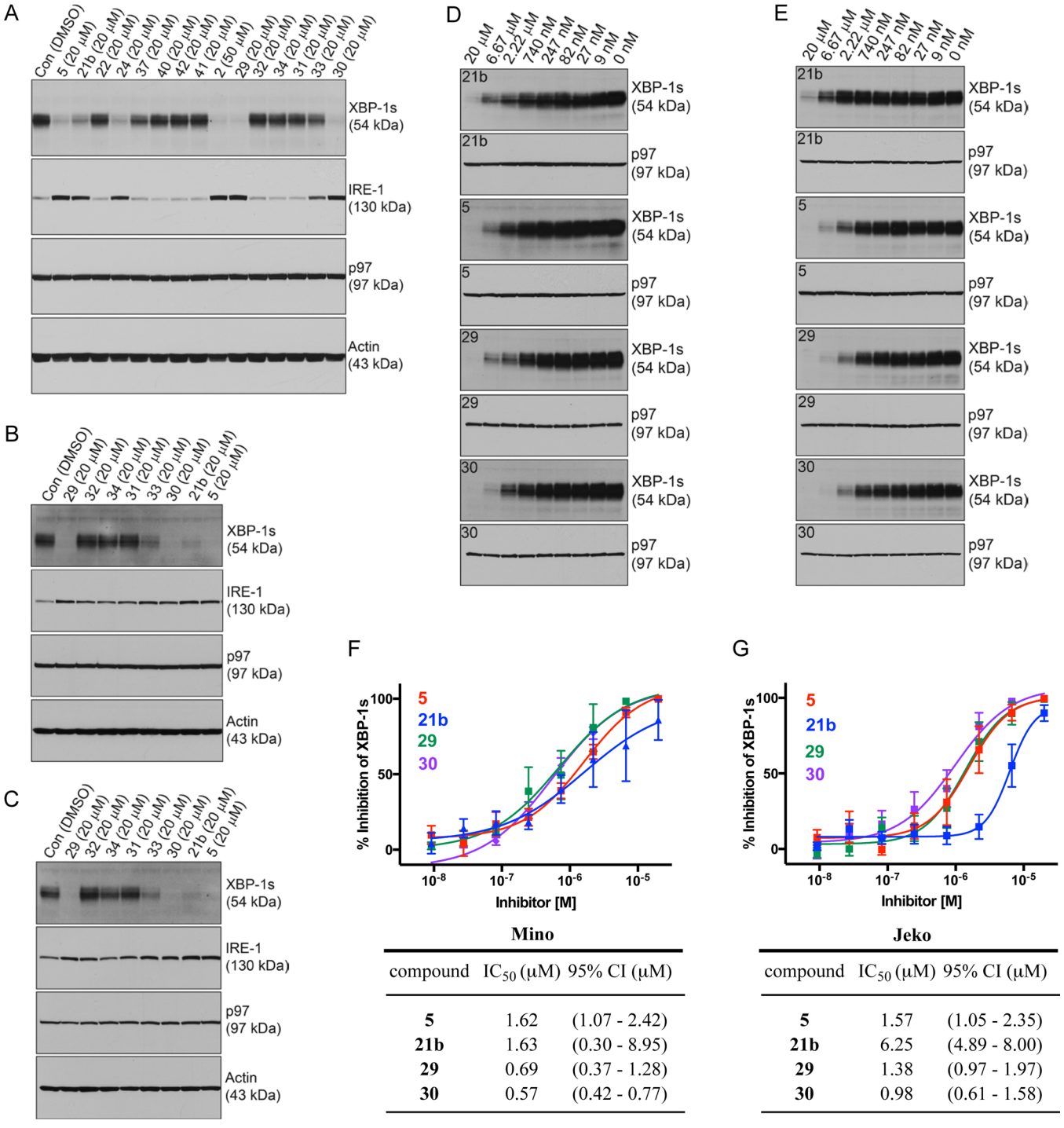

Mino

compound	IC_{50} (μM)	95% CI (μM)
5	1.62	(1.07 - 2.42)
21b	1.63	(0.30 - 8.95)
29	0.69	(0.37 - 1.28)
30	0.57	(0.42 - 0.77)

Jeko

compound	IC_{50} (μM)	95% CI (μM)
5	1.57	(1.05 - 2.35)
21b	6.25	(4.89 - 8.00)
29	1.38	(0.97 - 1.97)
30	0.98	(0.61 - 1.58)

Figure 5. Inhibition of XBP-1s expression in whole cells. (A) B cells were purified from the spleens of wild-type mice, stimulated with LPS for 48 h, treated with the indicated inhibitors at 20 μM for 24 h, lysed, and analyzed for expression of the indicated proteins by immunoblots. (B) Mino and (C) Jeko cells were treated with the indicated inhibitors at 20 μM for 24 h, lysed, and analyzed for the expression of indicated proteins by immunoblots. (D) Mino and (E) Jeko cells were treated with the indicated inhibitors at various doses for 48 h, lysed, and analyzed for the expression of indicated proteins by immunoblots. (F) Mino and (G) Jeko dose–response curves and IC_{50} values for inhibition of XBP-1s expression by indicated inhibitors as determined by immunoblots and densitometry (N = 3).

does treatment with 50 μM **2**. Despite their activity in the FRET-suppression assay, compounds **31**–**34** did not effectively inhibit XBP-1s expression in whole cells, presumably because of poor cell permeability and solubility. Compounds **37**, **40**, and **41**, which feature alternative electrophilic functional groups, similarly showed little to no inhibitory effect on XBP-1s expression in B cells at 20 μM. Consistent with previous results showing up-regulation of IRE-1 in response to XBP-1s deficiency[25] and suppression,[22] we observed an inverse correlation between pharmacological inhibition of XBP-1s and expression level of IRE-1 (Figure 5A).

The IRE-1/XBP-1 pathway is known to be critical for the survival multiple myeloma, malignancies derives from plasma cells.[14,26] However, the functional role of the ER stress

dx.doi.org/10.1021/jm5002452 | J. Med. Chem. 2014, 57, 4289–4301

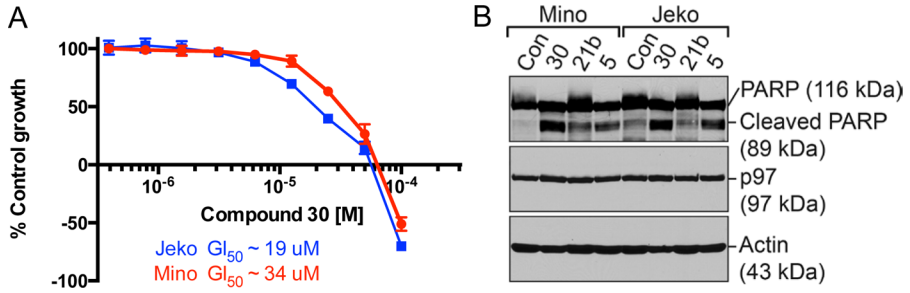

Figure 6. Growth inhibition and induction of apoptosis by **30**. (A) Human Mino and Jeko cells were cultured in the presence of **30** at various concentrations for 48 h and subjected to XTT assay. Percentages of cell growth were calculated relative to DMSO-treated (control) groups. (B) Human Mino and Jeko cells were cultured for 72 h in the presence of DMSO (control), **30** (50 μM), **21b** (50 μM), and **5** (50 μM). Cells were lysed for the analysis of the indicated proteins by immunoblot.

response in leukemia or lymphoma derived from mature B cells has been largely overlooked because leukemia and lymphoma cells do not expand their ER like that of multiple myeloma cells. We recently showed that chronic lymphocytic leukemia (CLL) growth and survival is highly dependent on the IRE-1/XBP-1 pathway and is inhibited by small molecules targeting IRE-1 RNase activity.[22] Mantle cell lymphoma (MCL) is an incurable non-Hodgkin's lymphoma developed from mantle zone-resident B cells. Since the role of the IRE-1/XBP-1 pathway in MCL is completely unknown, we examined the MCL cell lines Mino and Jeko for the expression of XBP-1s and discovered that XBP-1s is constitutively expressed by both. A subset of inhibitors was examined for inhibition of XBP-1s in these human MCL cell lines. As with wild-type mouse B cells, compounds **21b**, **29**, and **30** potently suppress the expression of XBP-1s and induce up-regulation of IRE-1 in Mino and Jeko cells. *N*-Isobutenyl derivative **33** also exhibits significant activity at 20 μM (Figure 5B and Figure 5C).

To establish the dependency of XBP-1s expression on inhibitor concentration, we used MCL cells to determine the whole cell IC_{50} values for **21b**, **29**, and **30**, in comparison to **5**, by immunoblots and densitometry (Figure 5D–G). Compound **30** proved to be the most potent inhibitor of XBP-1s expression in both Mino and Jeko cell lines (IC_{50} = 0.57 and 0.98 μM, respectively).

Lastly, we carried out XTT dose–response experiments to determine approximate GI_{50} concentrations for **30**, our most potent inhibitor of XBP-1s expression. After a 48 h treatment, **30** exhibited GI_{50} values of 34 and 19 μM in Mino and Jeko cells, respectively (Figure 6A). Total growth inhibition by **30** was achieved between 55 and 66 μM for these cell lines. We confirmed that growth inhibition is the result of apoptosis by treating Mino and Jeko cells with **30** for 72 h and analyzing cell lysates for cleaved PARP. Consistent with its superior potency in the suppression of XBP-1s, compound **30** induced PARP cleavage more strongly than either **21b** or **5** at 50 μM (Figure 6B). We also determined a GI_{50} value of ~34 μM in LPS-stimulated wild-type mouse B cells after treatment with **30** for 72 h (see Supporting Information). As expected, this result suggests that the growth of antibody-secreting plasma cells is also sensitive to inhibition of IRE-1 RNase activity.

CONCLUSION

We have described the synthesis and biological characterization of novel inhibitors of IRE-1. Although various salicylaldehydes have been reported to inhibit IRE-1 RNase activity in vitro, our results confirm that the presence of an *o*-hydroxy aromatic aldehyde is not sufficient for biological activity. In an effort toward functionalized derivatives of potent chromenone-based inhibitors, we prepared a series of carbamate substituted 2*H*-chromene-2-ones for further derivatization. Duff formylation of these substrates resulted in a tandem annelation reaction, giving rise to novel fused tricyclic scaffolds. Tetrahydrochromeno[3,4-*c*]pyridine **21b** served as a lead compound for the synthesis of a family of analogues.

Although replacement of the critical aldehyde group in **21b** with electrophilic surrogates diminished potency, some compounds retained weak to moderate inhibitory activity in vitro. Modifications to the phenol group in **21b** had a deleterious effect on potency in the FRET suppression assay, while changes at the distal N substituent were generally well tolerated. The ability of selected compounds to inhibit XBP-1s expression in wild-type B cells and human MCL cell lines highlights the importance of cell-based assays for this class of inhibitors, as a number of compounds with low- to mid-nanomolar activity in the FRET-suppression assay did not significantly reduce XBP-1s expression in whole cells. The *N*-methyl analogue **30** displayed an in vitro IRE-1 RNase IC_{50} value of 200 nM and potently inhibited the expression of XBP-1s in Mino and Jeko cells (IC_{50} = 0.57 and 0.98 μM, respectively). Compared to **21b**, compound **30** is also more effective at inducing apoptosis in MCL cells. The described tricyclic chromenones thus represent useful tool compounds for suppressing IRE-1 RNase activity in whole cells and for probing the importance of the IRE-1/XBP-1 pathway of the ER stress response in biological systems.

EXPERIMENTAL SECTION

General Synthesis Notes. Unless stated otherwise, reactions were performed in flame-dried glassware under a positive pressure of argon or nitrogen gas using dry solvents. Commercial grade reagents and solvents were used without further purification except where noted. Diethyl ether, toluene, dimethylformamide dichloromethane, and tetrahydrofuran were purified by a Glass Contour column-based solvent purification system. Other anhydrous solvents were purchased directly from chemical suppliers. Thin-layer chromatography (TLC) was performed using silica gel 60 F254 precoated plates (0.25 mm). Flash chromatography was performed using silica gel (60 μm particle size). The purity of all compounds was judged by TLC analysis (single spot/two solvent systems) using a UV lamp, CAM (ceric ammonium molybdate), ninhydrin, or basic $KMnO_4$ stain(s) for detection purposes. 1D and 2D NMR spectra were recorded on a Varian 400 MHz spectrometer. Proton chemical shifts are reported as δ values relative to residual signals from deuterated solvents ($CDCl_3$, CD_3OD, or DMSO-d_6). The purity of all assayed compounds was determined by RP-HPLC using an analytical C_{18} column with MeCN/water (0.1%

dx.doi.org/10.1021/jm5002452 | J. Med. Chem. 2014, 57, 4289–4301

formic acid) as eluent (4 mm × 150 mm column, 1 mL/min flow rate). All final compounds were determined to be between 95% and 98% pure. Compounds **2**, **5**, **8**, **10**–**12**, and **14** were purchased from commercial sources. Compounds **1** and **9** were synthesized as described previously.[22]

Procedure for Synthesis of β-Ketoesters 18a–d. A solution of the appropriate (*N*-Alloc) amino acid **17** (23.9 mmol) in 100 mL of DCM at 0 °C was treated with 2,2-dimethyl-1,3-dioxane-4,6-dione (4.47 g, 31.0 mmol), 4-dimethylaminopyridine (2.92 g, 23.9 mmol), and diisopropylcarbodiimide (3.70 mL, 23.9 mmol). The mixture was stirred from 0 °C to room temperature over 4 h, then washed with 10% aqueous $KHSO_4$ followed by brine. The organic layer was dried over Na_2SO_4 and concentrated. The resulting colorless liquid was dissolved in 50 mL of a 10:1 MeOH/toluene mixture and stirred at reflux for 15 h. After cooling, the mixture was concentrated under reduced pressure. Purification by flash column chromatography over silica gel (25%–60% EtOAc/hexanes) afforded **18a**, **18b**, and **18d** as colorless oils. Alkylidene pyrrolidine **18c** was obtained as a white solid.

Methyl 5-(((Allyloxy)carbonyl)amino)-3-oxobutanoate (18a). **18a** was obtained in 64% yield from **17a**. ^{1}H NMR (400 MHz, $CDCl_3$) δ 5.88 (ddt, J = 16.2, 10.7, 5.6 Hz, 1H), 5.49 (s, 1H), 5.29 (d, J = 17.2 Hz, 1H), 5.20 (d, J = 10.5 Hz, 1H), 4.56 (d, J = 5.5 Hz, 2H), 4.18 (d, J = 5.1 Hz, 2H), 3.72 (s, 3H), 3.50 (s, 2H); ^{13}C NMR (101 MHz, $CDCl_3$) δ 198.2. 167.0, 156.1, 132.5, 117.9, 66.0, 52.6, 50.8, 46.2; HRMS (ESI-TOF) m/z $[M + H]^+$ calcd for $C_9H_{14}NO_5$ 216.0867, found 216.0862.

Methyl 5-(((Allyloxy)carbonyl)amino)-3-oxopentanoate (18b). **18b** was obtained in 94% yield from **17b**. ^{1}H NMR (400 MHz, $CDCl_3$) δ 5.97–5.82 (m, 1H), 5.37–5.12 (m, 3H), 4.53 (d, J = 5.6 Hz, 2H), 3.73 (s, 3H), 3.50–3.37 (m, 4H), 2.80 (t, J = 5.7 Hz, 2H); ^{13}C NMR (101 MHz, $CDCl_3$) δ 202.2, 167.3, 156.2, 132.8, 132.8, 117.6, 117.5, 65.4, 52.4, 52.4, 48.9, 42.8, 35.3; HRMS (ESI-TOF) (m/z) $[M + H]^+$ calcd for $C_{10}H_{16}NO_5$ 230.10285, found 230.10297.

Allyl 2-(2-Methoxy-2-oxoethylidene)pyrrolidine-1-carboxylate (18c). **18c** was obtained in 56% yield from **17c**. ^{1}H NMR (400 MHz, $CDCl_3$) δ 6.52 (s, 1H), 5.94 (ddt, J = 17.2, 10.5, 5.7 Hz, 1H), 5.33 (d, J = 17.2 Hz, 1H), 5.25 (d, J = 10.4 Hz, 1H), 4.66 (d, J = 5.7 Hz, 2H), 3.73 (t, J = 7.2 Hz, 2H), 3.65 (s, 3H), 3.17 (t, J = 7.7 Hz, 2H), 1.91 (p, J = 7.5 Hz, 2H); ^{13}C NMR (101 MHz, $CDCl_3$) δ 169.2, 157.3, 152.6, 131.9, 118.5, 96.4, 66.6, 50.8, 49.5, 31.6, 21.1; HRMS (ESI-TOF) m/z $[M + H]^+$ calcd for $C_{11}H_{16}NO_4$ 226.1074, found 226.1068.

Methyl 7-(((Allyloxy)carbonyl)amino)-3-oxoheptanoate (18d). **18d** was obtained in 65% yield from **17d**. ^{1}H NMR (400 MHz, $CDCl_3$) δ 5.89 (ddt, J = 16.2, 10.7, 5.4 Hz, 1H), 5.28 (dd, J = 17.2, 1.5 Hz, 1H), 5.19 (dd, J = 10.4, 1.1 Hz, 1H), 4.82 (s, 1H), 4.53 (d, J = 5.5 Hz, 2H), 3.72 (s, 3H), 3.43 (s, 2H), 3.16 (dd, J = 12.9, 6.5 Hz, 2H), 2.56 (t, J = 7.1 Hz, 2H), 1.68–1.57 (m, 2H), 1.56–1.43 (m, 2H); ^{13}C NMR (101 MHz, $CDCl_3$) δ 202.4, 167.6, 156.3, 132.9, 117.6, 65.4, 52.4, 49.0, 42.4, 40.5, 29.1, 20.2; HRMS (ESI-TOF) m/z $[M + H]^+$ calcd for $C_{12}H_{20}NO_5$ 258.1336, found 258.1326.

General Procedure for Synthesis of Coumarins 19a–d. A solution of the appropriate β-keto ester **18** (10.1 mmol) in 50 mL of methanesulfonic acid at 0 °C was treated with resorcinol (1.11 g, 10.1 mmol) and stirred for 3.5 h. The mixture was poured into ice cold water, and the resulting yellow mixture was filtered. The filtrate was extracted with EtOAc and combined with the solids. The combined organic layer was concentrated and purified by flash chromatography over silica gel (0–20% MeOH/$CHCl_3$) to afford the pure coumarin derivatives **19a–d**.

Allyl (2-(7-Hydroxy-2-oxo-2*H*-chromen-4-yl)methyl)carbamate (19a). **19a** was obtained in 36% yield from **18a**. ^{1}H NMR (400 MHz, DMSO-d_6) δ 10.60 (s, 1H), 7.88 (t, J = 5.9 Hz, 1H), 7.64 (d, J = 8.7 Hz, 1H), 6.78 (d, J = 8.7 Hz, 1H), 6.73 (d, J = 2.3 Hz, 1H), 5.99 (s, 1H), 5.92 (ddt, J = 17.0, 10.6, 5.4 Hz, 1H), 5.29 (dd, J = 17.2, 1.6 Hz, 1H), 5.18 (d, J = 10.5 Hz, 1H), 4.52 (d, J = 5.3 Hz, 2H), 4.37 (d, J = 5.8 Hz, 2H); ^{13}C NMR (101 MHz, DMSO-d_6) δ 161.7, 160.8, 156.6, 155.4, 154.2, 134.0, 126.2, 117.6, 113.4, 110.3, 107.9, 102.8, 65.2, 41.0; HRMS (ESI-TOF) m/z $[M + H]^+$ calcd for $C_{13}H_{14}NO_5$ 276.0867, found 276.0863.

Allyl (2-(7-Hydroxy-2-oxo-2*H*-chromen-4-yl)ethyl)carbamate (19b). **19b** was obtained in 88% yield from **18b**. ^{1}H NMR (400 MHz, DMSO-d_6) δ 10.55 (s, 1H), 7.68 (d, J = 8.8 Hz, 1H), 7.40 (m, 1H), 6.80 (dd, J = 8.7, 2.3 Hz, 1H), 6.71 (d, J = 2.3 Hz, 1H), 6.07 (s, 1H), 5.99–5.78 (m, 1H), 5.24 (m, 1H), 5.15 (m, 1H), 4.45 (m, 2H), 3.29 (m, 2H), 2.87 (t, J = 6.7 Hz, 2H); ^{13}C NMR (101 MHz, DMSO-d_6) δ 161.1, 160.3, 156.0, 155.2, 154.2, 133.8, 133.7, 126.3, 116.9, 113.0, 111.3, 110.5, 110.4, 102.5, 102.4, 64.3, 31.5, 23.4; HRMS (ESI-TOF) (m/z) $[M + H]^+$ calcd for $C_{16}H_{16}NO_5$ 302.102 85, found 302.103 05.

Allyl (2-(7-Hydroxy-2-oxo-2*H*-chromen-4-yl)propyl)carbamate (19c). **19c** was obtained in 88% yield from **18c**. ^{1}H NMR (400 MHz, DMSO-d_6) δ 10.53 (s, 1H), 7.61 (d, J = 8.8 Hz, 1H), 7.33 (t, J = 5.5 Hz, 1H), 6.78 (d, J = 8.7, 1H), 6.69 (d, J = 2.4 Hz, 1H), 6.10 (s, 1H), 5.89 (ddt, J = 17.0, 10.6, 5.4 Hz, 1H), 5.25 (dd, J = 17.2, 1.6 Hz, 1H), 5.15 (d, J = 10.4 Hz, 1H), 4.45 (d, J = 5.3 Hz, 2H), 3.07 (q, J = 6.6 Hz, 2H), 2.72 (t, J = 7.6 Hz, 2H), 1.96–1.63 (m, 2H); ^{13}C NMR (101 MHz, DMSO- d_6) δ 161.5, 160.8, 157.0, 156.4, 155.6, 134.3, 126.7, 117.3, 113.3, 111.6, 109.9, 102.9, 64.6, 40.2, 28.7, 28.6; HRMS (ESI-TOF) m/z $[M + H]^+$ calcd for $C_{16}H_{18}NO_5$ 304.1180, found 304.1172.

Allyl (2-(7-Hydroxy-2-oxo-2*H*-chromen-4-yl)butyl)carbamate (19d). **19d** was obtained in 84% yield from **18d**. ^{1}H NMR (400 MHz, DMSO- d_6) δ 10.50 (s, 1H), 7.60 (d, J = 8.8 Hz, 1H), 7.21 (t, J = 5.7 Hz, 1H), 6.76 (d, J = 8.7 Hz, 1H), 6.67 (d, J = 2.4 Hz, 1H), 6.05 (s, 1H), 5.86 (ddt, J = 17.2, 10.5, 5.3 Hz, 1H), 5.22 (dd, J = 17.2, 1.7 Hz, 1H), 5.11 (dd, J = 10.4, 1.6 Hz, 1H), 4.42 (d, J = 5.3 Hz, 2H), 3.00 (d, J = 6.1 Hz, 2H), 2.69 (t, J = 7.4 Hz, 2H), 1.62–1.51 (m, 2H), 1.51–1.42 (m, 2H); ^{13}C NMR (101 MHz, DMSO-d_6) δ 161.5, 160.9, 157.5, 156.4, 155.5, 134.3, 126.8, 117.2, 113.3, 111.6, 109.7, 102.8, 64.5, 40.2, 31.0, 29.5, 25.8; HRMS (ESI-TOF) m/z $[M + H]^+$ calcd for $C_{17}H_{20}NO_5$ 318.1336, found 318.1339.

Duff Reaction Condition A. The appropriate coumarin derivative **19** (0.73 mmol) in 9 mL of AcOH was treated with HMTA (255 mg, 1.82 mmol) and stirred for 18 h at 95 °C. The reaction mixture was concentrated, and the resulting slurry was dissolved in 12 mL of a 1:1 1 M aqueous HCl/EtOAc solution and stirred at 60 °C for 2 h. The organic layer was separated, and the aqueous layer was extracted with EtOAc. The combined organic layers were washed with water, dried with $MgSO_4$, and concentrated. Purification by silica gel flash column chromatography (EtOAc/hexane) afforded the desired bicyclic formyl derivatives **20a–d**.

Duff Reaction Condition B. The appropriate coumarin derivative **19** (0.73 mmol) in 3 mL of TFA was treated with HMTA (255 mg, 1.82 mmol) and stirred for 18 h at 75 °C. The reaction mixture was concentrated, and the resulting slurry was dissolved in 12 mL of a 1:1 1 M aqueous HCl/EtOAc solution and stirred at 60 °C for 2 h. The organic layer was separated, and the aqueous layer was extracted with EtOAc. The combined organic layers were washed with water, dried with $MgSO_4$, and concentrated. Purification by silica gel flash column chromatography (EtOAc/hexane) afforded the desired bicyclic and tricyclic formyl derivatives.

Duff Reaction Condition C. The appropriate coumarin derivative **19** (0.47 mmol) in 15 mL of MeCN was treated with pyridine (18.5 mg, 0.23 mmol) and acetic anhydride (239 mg, 2.35 mmol). After being stirred for 6 h at room temperature, the mixture was diluted with brine and extracted with EtOAc. The organic layer was dried with $MgSO_4$ and concentrated. The resulting crude product dissolved in 2 mL of TFA was treated with HMTA (164 mg, 1.17 mmol) and stirred for 18 h at 95 °C. The reaction mixture was concentrated, and the resulting slurry was dissolved in 12 mL of a 1:1 1 M aqueous HCl/EtOAc solution and stirred at 60 °C for 2 h. The organic layer was separated, and the aqueous layer was extracted with EtOAc. The combined organic layers were washed with water, dried with $MgSO_4$, and concentrated. Purification by silica gel flash column chromatography (EtOAc/hexane) afforded the desired bicyclic and tricyclic formyl derivatives.

dx.doi.org/10.1021/jm5002452 | J. Med. Chem. 2014, 57, 4289–4301

Allyl (2-(8-Formyl-7-hydroxy-2-oxo-2*H*-chromen-4-yl)-methyl)carbamate (20a). **20a** was obtained in 4% yield (methods A, B, and C) from **19a**. ^{1}H NMR (400 MHz, $CDCl_3$) δ 12.24 (s, 1H), 10.60 (s, 1H), 7.73 (d, J = 9.0 Hz, 1H), 6.91 (d, J = 9.0 Hz, 1H), 6.32 (s, 1H), 5.94 (ddt, J = 16.5, 11.1, 5.8 Hz, 1H), 5.34 (d, J = 17.2 Hz, 1H), 5.27 (d, J = 10.3 Hz, 1H), 5.19 (t, J = 5.6 Hz, 1H), 4.64 (dt, J = 5.7, 1.4 Hz, 2H), 4.54 (d, J = 6.3 Hz, 2H); ^{13}C NMR (101 MHz, $CDCl_3$) δ 193.3, 165.4, 159.1, 156.3, 156.1, 152.1, 132.2, 131.8, 118.5, 114.7, 109.74, 109.71, 108.8, 66.4, 41.3; HRMS (ESI-TOF) m/z $[M + H]^+$ calcd for $C_{15}H_{14}NO_6$ 304.0816, found 304.0820.

Allyl (2-(8-Formyl-7-hydroxy-2-oxo-2*H*-chromen-4-yl)ethyl)-carbamate (20b). **20b** was obtained in 10% yield (method A) from **19b**. ^{1}H NMR (400 MHz, $CDCl_3$) δ 12.24 (s, 1H), 10.60 (s, 1H), 7.92 (d, J = 9.1 Hz, 1H), 6.93 (d, J = 9.0 Hz, 1H), 6.19 (s, 1H), 5.90 (m, 1H), 5.39−5.15 (m, 2H), 5.03 (bs, 1H), 4.58 (m, 2H), 3.49 (m, 2H), 2.99 (t, J = 7.2 Hz, 2H); ^{13}C NMR (101 MHz, $CDCl_3$) δ 193.5, 193.4, 165.5, 159.2, 156.6, 156.5, 153.4, 133.1, 132.6, 118.2, 114.8, 112.2, 112.1, 111.1, 109.0, 66.0, 40.1, 32.8; HRMS (ESI-TOF) (m/z) $[M + H]^+$ calcd for $C_{16}H_{16}NO_6$ 318.097 77, found 318.097 46.

Allyl (2-(8-Formyl-7-hydroxy-2-oxo-2*H*-chromen-4-yl)-propyl)carbamate (20c). **20c** was obtained in 13% yield (method A) from **19c**. ^{1}H NMR (400 MHz, $CDCl_3$) δ 12.20 (s, 1H), 10.58 (s, 1H), 7.72 (d, J = 9.0 Hz, 1H), 6.88 (d, J = 9.0 Hz, 1H), 6.19 (s, 1H), 5.90 (ddt, J = 16.8, 11.1, 5.6 Hz, 1H), 5.29 (dd, J = 17.2, 1.5 Hz, 1H), 5.20 (dd, J = 10.4, 1.2 Hz, 1H), 4.98 (t, J = 5.2 Hz, 1H), 4.56 (d, J = 5.4 Hz, 2H), 3.33 (q, J = 6.5 Hz, 2H), 2.98−2.59 (m, 2H), 1.90 (tt, J = 13.7, 6.9 Hz, 2H); ^{13}C NMR (101 MHz, $CDCl_3$) δ 193.4, 165.2, 159.3, 156.4, 156.3, 155.6, 132.7, 132.5, 117.9, 114.4, 111.0, 110.9, 108.8, 65.7, 40.4, 29.1, 28.5; HRMS (ESI-TOF) m/z $[M + H]^+$ calcd for $C_{17}H_{18}NO_6$ 332.1129, found 332.1128.

Allyl (2-(8-Formyl-7-hydroxy-2-oxo-2*H*-chromen-4-yl)butyl)-carbamate (20d). **20d** was obtained in 15% yield (method A) from **19d**. ^{1}H NMR (400 MHz, $CDCl_3$) δ 12.22 (s, 1H), 10.60 (s, 1H), 7.74 (d, J = 9.0 Hz, 1H), 6.89 (d, J = 9.0 Hz, 1H), 6.17 (s, 1H), 5.90 (ddt, J = 16.1, 10.8, 5.7 Hz, 1H), 5.29 (dd, J = 17.2, 1.6 Hz, 1H), 5.20 (dd, J = 10.4, 1.3 Hz, 1H), 4.80 (s, 1H), 4.55 (d, J = 5.6 Hz, 2H), 3.26 (q, J = 6.4 Hz, 2H), 2.93−2.56 (m, 2H), 1.78−1.56 (m, 4H); ^{13}C NMR (101 MHz, $CDCl_3$) δ 139.4, 165.2, 159.4, 156.38, 156.37, 156.1, 132.8, 132.7, 117.8, 114.4, 111.1, 111.0, 109.8, 65.6, 40.3, 31.5, 29.9, 25.2; HRMS (ESI-TOF) m/z $[M + H]^+$ calcd for $C_{18}H_{20}NO_6$ 346.1285, found 346.1288.

Allyl 7-Formyl-8-hydroxy-5-oxo-4,5-dihydro-1*H*-chromeno-[3,4-*c*]pyridine-3(2*H*)-carboxylate (21b). **21b** was obtained in 22% (method B) and 41% (method C) yield from **19b**. ^{1}H NMR (400 MHz, $CDCl_3$) δ 12.15 (s, 1H), 10.61 (s, 1H), 7.68 (d, J = 8.4 Hz, 1H), 6.92 (d, J = 9.0 Hz, 1H), 5.94 (m, 1H), 5.33 (m, 1H), 5.24 (m, 1H), 4.64 (d, J = 5.7 Hz, 2H), 4.47 (m, 2H), 3.81 (t, J = 5.8 Hz, 2H), 2.86 (m, 2H); ^{13}C NMR (101 MHz, $CDCl_3$) δ 193.3, 164.9, 158.4, 155.2, 154.7, 146.4, 132.7, 131.8, 118.3, 117.2, 114.8, 111.2, 108.7, 66.7, 41.9, 39.2, 24.9; HRMS (ESI-TOF) (m/z) $[M + H]^+$ calcd for $C_{17}H_{16}NO_6$ 330.097 21, found 330.096 24.

Allyl 8-Formyl-9-hydroxy-6-oxo-2,3,5,6-tetrahydrochromeno[3,4-*c*]azepine-4(1*H*)-carboxylate (21c). **21c** was obtained in 18% (method B) and 17% (method C) yield from **19c**. ^{1}H NMR (400 MHz, $CDCl_3$) δ 12.17 (s, 1H), 10.61 (s, 1H), 7.79 (d, J = 9.2 Hz, 1H), 6.90 (d, J = 8.9 Hz, 1H), 5.87 (ddt, J = 16.3, 10.8, 5.3 Hz, 1H), 5.28 (dd, J = 17.2, 1.5 Hz, 1H), 5.16 (d, J = 10.8 Hz, 1H), 4.65 (s, 2H), 4.55 (d, J = 5.1 Hz, 2H), 3.98−3.57 (m, 2H), 3.08−2.96 (m, 2H), 2.13−2.00 (m, 2H); ^{13}C NMR (101 MHz, $CDCl_3$) δ 193.4, 164.8, 159.3, 155.7, 155.0, 152.2, 132.54, 132.50, 122.0, 117.3, 114.4, 111.9, 108.6, 66.3, 47.8, 42.9, 27.6, 24.6; HRMS (ESI-TOF) m/z $[M + H]^+$ calcd for $C_{18}H_{18}NO_6$ 344.1129, found 344.1137.

Allyl 9-Formyl-10-hydroxy-7-oxo-2,3,5,6-tetrahydro-1*H*-chromeno[3,4-*d*]azocine-4(7*H*)-carboxylate (21d). **21d** was obtained in 3% (method B) and 9% (method C) yield from **19d**. ^{1}H NMR (400 MHz, $CDCl_3$) δ 12.18 (s, 1H), 10.61 (s, 1H), 7.78 (d, J = 8.6 Hz, 1H), 6.91 (d, J = 8.9 Hz, 1H), 5.95 (ddt, J = 16.9, 10.8, 5.6 Hz, 1H), 5.32 (d, J = 17.1 Hz, 1H), 5.21 (d, J = 10.3 Hz, 1H), 4.66 (s, 2H), 4.64 (d, J = 4.7 Hz, 2H), 3.62−3.49 (m, 2H), 3.07−2.96 (m, 2H), 1.92−1.80 (m, 2H), 1.80−1.69 (m, 2H); ^{13}C NMR (101 MHz, $CDCl_3$) δ 139.3, 164.8, 159.1, 155.8, 155.5, 152.0, 132.9, 132.6, 119.5, 117.6, 114.5, 111.3, 108.7, 66.5, 46.2, 44.4, 26.1, 25.7, 25.1; HRMS (ESI-TOF) m/z $[M + H]^+$ calcd for $C_{19}H_{20}NO_6$ 358.1285, found 358.1290.

Allyl 8-Hydroxy-7-(hydroxymethyl)-5-oxo-4,5-dihydro-1*H*-chromeno[3,4-*c*]pyridine-3(2*H*)-carboxylate (22). Compound **21b** (24 mg, 73 μmol) in 2 mL of MeOH at 0 °C was treated with sodium borohydride (3.0 mg, 73 μmol) and stirred for 40 min. The reaction was quenched with 1 M aqueous HCl and extracted with EtOAc. The organic layers were dried over Na_2SO_4 and concentrated. Purification by flash column chromatography over silica gel (40% −50% EtOAc/hexane) afforded **22** as a white foam (16 mg, 66%). ^{1}H NMR (400 MHz, $CDCl_3$) δ 9.65 (bs, 1H), 7.35 (d, J = 8.4 Hz, 1H), 6.85 (d, J = 8.7 Hz, 1H), 5.94 (m, J = 11.1, 5.6 Hz, 1H), 5.33 (m, 3H), 5.24 (m, 1H), 4.64 (m, 2H), 4.40 (s, 2H), 3.77 (t, J = 5.7 Hz, 2H), 2.84 (m, 2H); ^{13}C NMR (101 MHz, $CDCl_3$) δ 180.6, 160.4, 149.8, 147.8, 132.7, 123.5, 118.2, 114.7, 111.8, 111.1, 66.7, 59.0, 41.8, 39.3, 24.9; HRMS (ESI-TOF) (m/z) $[M + H]^+$ calcd for $C_{17}H_{18}NO_6$ 332.113 42, found 332.114 73.

Allyl 8-Hydroxy-7-chloro-5-oxo-4,5-dihydro-1*H*-chromeno-[3,4-*c*]pyridine-3(2*H*)-carboxylate (23). Compound **22** (17 mg, 51 μmol) in 2 mL of DCM at room temperature was treated with thionyl chloride (19 μL, 257 μmol) and stirred for 5.5 h. The reaction was diluted with DCM and washed with saturated aqueous NH_4Cl, dried over Na_2SO_4, and concentrated under reduced pressure. The resulting white solid **23** was suffiently pure by NMR and HPLC analysis for further use (12 mg, 67%). ^{1}H NMR (400 MHz, $CDCl_3$) δ 9.42 (m, 0.5H), 7.69 (m, 0.5H), 7.38 (m, 1H), 6.89 (m, 1H), 5.95 (m, 1H), 5.30 (m, 3H), 4.91 (s, 1H), 4.65 (m, 2H), 4.44 (d, J = 17.7 Hz, 2H), 3.79 (m, 2H), 2.85 (m, 2H); ^{13}C NMR (101 MHz, $CDCl_3$) δ 160.3, 157.9, 151.5, 149.9, 132.7, 124.7, 123.6, 118.3, 114.5, 113.1, 112.7, 112.3, 111.9, 111.2, 66.8, 58.9, 42.0, 39.4, 34.3, 29.8, 24.8; HRMS (ESI-TOF) (m/z) $[M + H]^+$ calcd for $C_{17}H_{16}ClNO_5$ 350.078 98, found 346.128 50 (observed mass corresponds to the 7-methoxymethyl derivative, resulting from displacement of the chloride with methanol during LCMS).

Allyl 7-(1,3-Dioxan-2-yl)-8-hydroxy-5-oxo-4,5-dihydro-1*H*-chromeno[3,4-*c*]pyridine-3(2*H*)-carboxylate (24). A solution of **21b** in (150 mg, 455 μmol) in 4 mL of benzene was treated with 1,3-propanediol (99.0 μL, 1.40 mmol) and *p*-toluenesulfonic acid monohydrate (4.3 mg, 23 μmol) and stirred for 2 h. The reaction was quenched with 2 drops of NEt_3, diluted with EtOAc, and washed with brine. The organic layer was dried over Na_2SO_4 and concentrated. Purification by flash column chromatography over silica gel (30%−50% EtOAc/hexanes eluent) afforded **24** as a yellow solid (157 mg, 89%). ^{1}H NMR (400 MHz, $CDCl_3$) δ 8.82 (s, 1H), 7.36 (d, J = 8.2 Hz, 1H), 6.79 (d, J = 8.8 Hz, 1H), 6.28 (s, 1H), 5.91 (m, 1H), 5.30 (m, 1H), 5.20 (m, 1H), 4.61 (d, J = 5.6 Hz, 2H), 4.39 (s, 2H), 4.28 (dd, J = 11.6, J = 4.6 Hz, 2H), 4.09 (m, 2H), 3.74 (t, J = 5.8 Hz, 2H), 2.79 (m, 2H), 2.26 (m, 1H), 1.53 (m, 1H); ^{13}C NMR (101 MHz, $CDCl_3$) δ 159.5, 159.3, 155.2, 150.5, 146.6, 132.8, 125.3, 118.0, 116.3, 114.5, 111.8, 109.9, 98.1, 67.9, 66.5, 41.8, 39.3, 25.8, 24.7; HRMS (ESI-TOF) (m/z) $[M + H]^+$ calcd for $C_{20}H_{22}NO_7$ 388.139 08, found 388.138 10.

Allyl 7-(1,3-Dithian-2-yl)-8-hydroxy-5-oxo-4,5-dihydro-1*H*-chromeno[3,4-*c*]pyridine-3(2*H*)-carboxylate (25). Compound **21b** (39.0 mg, 118 μmol) and 1,3-propanedithiol (13.0 μL, 130 μmol) in 2.5 mL of DCM at room temperature were treated with BF_3·OEt_2 (6.0 μL, 47 μmol) and stirred for 17 h. The reaction was quenched with saturated aqueous $NaHCO_3$, and the aqueous layer was extracted with EtOAc. The combined organic layers were dried over Na_2SO_4 and concentrated under reduced pressure. Purification by flash column chromatography over silica gel (25−50% EtOAc/hexane) afforded **25** as a white foam (39 mg, 79%). ^{1}H NMR (400 MHz, $CDCl_3$) δ 7.55 (s, 1H), 7.43 (d, J = 8.4 Hz, 1H), 6.91 (d, J = 8.9 Hz, 1H), 6.26 (s, 1H), 5.95 (m, 1H), 5.33 (m, 1H), 5.24 (m, 1H), 4.64 (m, 2H), 4.47 (m, 2H), 3.78 (t, J = 5.8 Hz, 2H), 3.17 (m, 2H), 2.91 (m, 4H), 2.24 (m, 1H), 1.94 (m, 1H); ^{13}C NMR (101 MHz, $CDCl_3$) δ 159.5, 155.3, 149.8, 146.9, 132.8, 124.8, 118.1, 116.7, 114.9, 112.5,

dx.doi.org/10.1021/jm5002452 | *J. Med. Chem.* 2014, 57, 4289−4301

111.1, 110.6, 77.5, 77.2, 76.8, 66.6, 42.0, 39.2, 37.4, 31.3, 24.9, 24.7, 23.0, 14.3, 14.3. HRMS (ESI-TOF) (m/z) $[M + H]^+$ calcd for $C_{20}H_{22}NO_5S_2$ 420.093 99, found 420.092 48.

Allyl 7-Formyl-8-methoxy-5-oxo-4,5-dihydro-1*H*-chromeno-[3,4-*c*]pyridine-3(2*H*)-carboxylate (26). A solution of **24** (20 mg, 52 μmol) in 1 mL of DMF was treated with K_2CO_3 (36 mg, 258 μmol) followed by iodomethane (10 μL, 155 μmol). After being stirred at room temperature for 18 h, the mixture was diluted with saturated aqueous NH_4Cl, extracted with DCM, and concentrated to dryness. The residue was taken up in 500 μL of dioxane, treated with 2 mL of 4 M aqueous HCl, and stirred at room temperature for 30 min. The mixture was diluted with water and extracted with DCM. The combined organic layers were dried over Na_2SO_4 and concentrated under reduced pressure. Purification by flash column chromatography over silica gel (0−10% MeOH/$CHCl_3$) afforded **26** as a white powder (12 mg, 67%). ^{1}H NMR (400 MHz, $CDCl_3$) δ 10.68 (s, 1H), 7.71 (d, J = 8.7 Hz, 1H), 6.98 (d, J = 9.0 Hz, 1H), 5.95 (m, 1H), 5.33 (m, 1H), 5.24 (m, 1H), 4.65 (m, 2H), 4.48 (s, 2H), 4.01 (s, 3H), 3.82 (t, J = 5.8 Hz, 2H), 2.87 (m, 2H); ^{13}C NMR (101 MHz, $CDCl_3$) δ 187.2, 162.6, 158.6, 157.2, 155.3, 145.7, 132.8, 132.7, 132.7, 129.7, 118.3, 118.2, 112.9, 112.7, 108.2, 66.7, 56.8, 42.0, 39.3, 29.9, 24.9; HRMS (ESI-TOF) (m/z) $[M + H]^+$ calcd for $C_{18}H_{18}NO_6$ 344.113 41, found 344.114 32.

Allyl 7-Formyl-8-benzyloxy-5-oxo-4,5-dihydro-1*H*-chromeno[3,4-*c*]pyridine-3(2*H*)-carboxylate (27). A solution of **24** (20 mg, 52 μmol) in 1 mL of DMF was treated with K_2CO_3 (36 mg, 260 μmol) followed by benzyl bromide (9.0 μL, 78 μmol). After being stirred at room temperature for 18 h, the mixture was diluted with saturated aqueous NH_4Cl, extracted with DCM, and concentrated to dryness. The residue was taken up in 500 μL of dioxane, treated with 2 mL of 4 N aqueous HCl, and stirred at room temperature 30 min. The mixture was diluted with water and extracted with DCM. The combined organic layers were dried over Na_2SO_4 and concentrated under reduced pressure. Purification by flash column chromatography over silica gel (0−10% MeOH/$CHCl_3$) afforded **27** as a white powder (18 mg, 72%). ^{1}H NMR (400 MHz, $CDCl_3$) δ 10.72 (d, J = 5.4 Hz, 1H), 7.67 (d, J = 8.6 Hz, 1H), 7.58−7.31 (m, 5H), 7.01 (d, J = 9.0 Hz, 1H), 5.95 (m, 1H), 5.35 (m, 0.5H), 5.30 (m, 2.5H), 5.24 (m, 1H), 4.65 (m, 2H), 4.47 (s, 2H), 3.81 (t, J = 5.8 Hz, 2H), 2.87 (m, 2H); ^{13}C NMR (101 MHz, $CDCl_3$) δ 187.1, 161.7, 158.7, 154.0, 145.6, 135.4, 132.7, 129.5, 128.9, 128.5, 127.0, 118.3, 113.2, 113.1, 109.6, 71.2, 66.7, 51.3, 42.0, 39.2, 29.8, 24.8; HRMS (ESI-TOF) (m/z) $[M + H]^+$ calcd for $C_{24}H_{22}NO_6$ 420.144 71, found 420.145 29.

7-(1,3-Dioxan-2-yl)-8-hydroxy-3,4-dihydro-1*H*-chromeno-[3,4-*c*]pyridin-5(2*H*)-one (28). A solution of **24** (70 mg, 180 μmol) in 4 mL of DCM at room temperature was treated with phenylsilane (67 mg, 540 μmol) and tetrakis(triphenylphosphine)palladium(0) (10 mg, 9.0 μmol) and stirred at room temperature for 25 min. The mixture was concentrated and the residue purified by flash chromatography over silica gel (0%−10% MeOH/$CHCl_3$) to afford **28** as a yellow solid (54 mg, 98%). ^{1}H NMR (400 MHz, $CDCl_3$) δ 7.35 (d, J = 8.8 Hz, 1H), 6.78 (d, J = 8.8 Hz, 1H), 6.28 (s, 1H), 4.24 (m, 2H), 4.06 (m, 2H), 3.75 (m, 2H), 3.11 (t, J = 5.8 Hz, 2H), 2.70 (m, 2H), 2.36−2.11 (m, 1H), 1.92 (bs, 1H), 1.50 (m, 1H); ^{13}C NMR (101 MHz, $CDCl_3$) δ 160.2, 159.0, 150.6, 146.8, 135.0, 125.1, 119.0, 114.3, 112.5, 109.9, 98.3, 68.0, 43.4, 42.0, 25.9, 25.3; HRMS (ESI-TOF) (m/z) $[M + H]^+$ calcd for $C_{16}H_{18}NO_5$ 304.117 95, found 304.117 82.

3-Acetyl-8-hydroxy-5-oxo-2,3,4,5-tetrahydro-1*H*-chromeno-[3,4-*c*]pyridine-7-carbaldehyde (29). A solution of **28** (20 mg, 66 μmol) in 1 mL of DCM was treated with pyridine (11 μL, 130 μmol) and acetyl chloride (7.0 μL, 99 μmol), then stirred at room temperature for 20 min. After concentration under reduced pressure, the residue was taken up in 500 μL of dioxane, treated with 2 mL of 4 M aqueous HCl, and stirred at room temperature for 30 min. The mixture was diluted with water and extracted with DCM. The combined organic layers were dried over Na_2SO_4 and concentrated under reduced pressure. Purification by flash column chromatography over silica gel (0−10% MeOH/$CHCl_3$) afforded **29** as a white powder (17 mg, 90%). ^{1}H NMR (400 MHz, DMSO-d_6) δ 11.84 (s, 1H), 10.46 (s, 1H), 7.90 (m (rotomer), 1H), 7.00 (d, J = 8.9 Hz, 1H), 4.32 (m, 2H), 3.73 (t, J = 5.7 Hz, 2H), 2.96 (m, 2H), 2.83 (m, 1H), 2.10 (m (rotomer), 3H); ^{13}C NMR (101 MHz, DMSO-d_6) δ 191.1, 191.0, 168.9, 163.2, 163.1, 158.2, 153.5, 147.0, 146.8, 132.2, 116.7, 116.5, 113.9, 111.1, 109.1, 104.6, 43.2, 41.4, 36.3, 25.0, 24.3, 21.8, 21.3; HRMS (ESI-TOF) (m/z) $[M + H]^+$ calcd $C_{15}H_{14}NO_5$ 288.087 20, found 288.086 54.

8-Hydroxy-3-methyl-5-oxo-2,3,4,5-tetrahydro-1*H*-chromeno[3,4-*c*]pyridine-7-carbaldehyde (30). A solution of **28** (50.0 mg, 165 μM) in 2 mL of 1:1 dioxane/THF was treated with 37% aqueous formaldehyde (27.0 μL, 330 μM), 10% Pd/C (40 mg), placed under H_2 atmosphere, and stirred at room temperature for 3 h. The mixture was filtered through Celite with MeOH rinsing and concentrated to afford the crude methylamine. The residue was taken up in 500 μL of dioxane, treated with 2 mL of 4 M aqueous HCl, and stirred at room temperature 30 min. The mixture was diluted with water and extracted with DCM. The combined organic layers were dried over Na_2SO_4 and concentrated under reduced pressure. Purification by flash column chromatography over silica gel (0−10% MeOH/$CHCl_3$) afforded **30** as a white powder (35 mg, 67%). ^{1}H NMR (400 MHz, $CDCl_3$) δ 12.15 (s, 1H), 10.61 (s, 1H), 7.66 (d, J = 9.0 Hz, 1H), 6.92 (d, J = 9.0 Hz, 1H), 3.59 (s, 2H), 3.03−2.97 (m, 2H), 2.97−2.90 (m, 2H), 2.64 (s, 3H); ^{13}C NMR (101 MHz, $CDCl_3$) δ 193.2, 164.8, 158.4, 154.6, 145.5, 131.7, 117.3, 114.6, 111.0, 108.6, 51.6, 50.2, 45.0, 25.3; HRMS (ESI-TOF) m/z $[M + H]^+$ calcd for $C_{14}H_{14}NO_4$ 260.0917, found 260.0915.

3-Benzyl-8-hydroxy-5-oxo-2,3,4,5-tetrahydro-1*H*-chromeno[3,4-*c*]pyridine-7-carbaldehyde (31). A solution of **28** (20 mg, 66 μmol) in 1.5 mL of DMF at room temperature was treated with NEt_3 (10 mg, 99 μmol) and benzyl bromide (12 mg, 73 μmol). After being stirred for 5 h, the mixture was concentrated and treated with 4 mL of 4 M aqueous HCl and stirred for 1 h. The mixture was adjusted to pH 7 with 10% aqueous Na_2CO_3, extracted with DCM, dried over $MgSO_4$, and concentrated. Purification by silica gel flash column chromatography (MeOH/$CHCl_3$) gave **31** as a white solid (15.4 mg, 70%). ^{1}H NMR (400 MHz, $CDCl_3$) δ 12.15 (s, 1H), 10.61 (s, 1H), 7.65 (d, J = 9.0 Hz, 1H), 7.42−7.30 (m, 5H), 6.90 (d, J = 9.0 Hz, 1H), 3.87 (s, 2H), 3.59 (s, 2H), 2.94 (s, 4H); ^{13}C NMR (101 MHz, $CDCl_3$) δ 193.3, 164.5, 158.8, 154.5, 146.2, 137.1, 131.7, 129.2, 128.5, 127.6, 119.0, 114.3, 111.5, 108.5, 62.3, 50.1, 48.0, 26.0; HRMS (ESI-TOF) m/z $[M + H]^+$ calcd for $C_{20}H_{18}NO_4$ 336.1230, found 336.1224.

3-(4-Fluorobenzyl)-8-hydroxy-5-oxo-2,3,4,5-tetrahydro-1*H*-chromeno[3,4-*c*]pyridine-7-carbaldehyde (32). A solution of **28** (20 mg, 66 μmol) in 1.5 mL of DMF at room temperature was treated with NEt_3 (10 mg, 99 μmol) and 4-fluorobenzyl bromide (12 mg, 73 μmol). After being stirred for 5 h, the mixture was concentrated and treated with 4 mL of 4 M aqueous HCl and stirred for 1 h. The mixture was adjusted to pH 7 with 10% aqueous Na_2CO_3, extracted with DCM, dried over $MgSO_4$, and concentrated. Purification by silica gel flash column chromatography (MeOH/$CHCl_3$) gave **32** as a pale yellow solid (12 mg, 49%). ^{1}H NMR (400 MHz, $CDCl_3$) δ 12.15 (s, 1H), 10.62 (s, 1H), 7.66 (d, J = 9.0 Hz, 1H), 7.36 (m, 2H), 7.06 (m, 2H), 6.86 (m, 1H), 3.70 (bs, 2H), 3.51 (m, 2H), 2.86 (m, 4H); ^{13}C NMR (101 MHz, $CDCl_3$) δ 193.4, 164.7, 158.8, 156.3, 154.7, 146.2, 143.8, 131.9, 131.0, 127.9, 125.4, 115.7, 115.5, 114.6, 114.0, 111.5, 108.7, 68.7, 68.0, 61.5, 50.4, 48.1, 31.2, 29.9, 26.0; HRMS (ESI-TOF) m/z $[M + H]^+$ calcd for $C_{20}H_{17}FNO_4$ 354.114 16, found 354.114 38.

8-Hydroxy-3-(2-methylallyl)-5-oxo-2,3,4,5-tetrahydro-1*H*-chromeno[3,4-*c*]pyridine-7-carbaldehyde (33). A solution of **28** (20 mg, 67 μmol) in 1.5 mL of DMF at room temperature was treated with NEt_3 (10 mg, 99 μmol) and 3-bromo-2-methylpropene (9.9 mg, 74 μmol). After being stirred for 5 h, the mixture was concentrated and treated with 4 mL of 4 M aqueous HCl and stirred for 1 h. The mixture was adjusted to pH 7 with 10% aqueous Na_2CO_3, extracted with DCM, dried over $MgSO_4$, and concentrated. Purification by silica gel flash column chromatography (MeOH/$CHCl_3$) gave **33** as a yellow solid (15 mg, 75%). ^{1}H NMR (400 MHz, $CDCl_3$) δ 12.14 (s, 1H), 10.61 (s, 1H), 7.66 (d, J = 9.0 Hz, 1H), 6.90 (d, J = 9.0 Hz, 1H),

dx.doi.org/10.1021/jm5002452 | J. Med. Chem. 2014, 57, 4289−4301

5.01 (s, 2H), 3.52 (s, 2H), 3.22 (s, 2H), 2.94 (s, 2H), 2.87 (s, 2H), 1.81 (s, 3H); ^{13}C NMR (101 MHz, $CDCl_3$) δ 193.2, 164.6, 158.6, 154.6, 146.0, 140.5, 131.7, 115.3, 114.5, 111.3, 108.5, 105.0, 64.4, 50.2, 48.0, 25.6, 20.8; HRMS (ESI-TOF) m/z $[M + H]^+$ calcd for $C_{17}H_{18}NO_4$ 300.1230, found 300.1223.

7-Formyl-8-hydroxy-5-oxo-4,5-dihydro-1*H*-chromeno[3,4-*c*]pyridine-3(2*H*)-carboximidamide (34). A solution of **28** (20 mg, 66 μmol) in 1 mL of DCM was treated with NEt_3 (28 μL, 198 μmol) followed by 1,3-di-Boc-2-(trifluoromethylsulfonyl)guanidine (58 mg, 146 μmol) and stirred at room temperature for 18 h. The mixture was diluted with saturated aqueous NH_4Cl and extracted with DCM. The combined organic layers were dried over Na_2SO_4 and concentrated under reduced pressure. Purification by flash column chromatography over silica gel (40% EtOAc/hexanes) gave the guanidinylated intermediate as a glassy solid. The material was then treated with 2 mL of a 1:1 TFA/DCM solution and stirred at room temperature for 4 h. The mixture was concentrated to remove TFA, and the resulting solid was washed with three portions of DCM. Drying of the solid under vacuum afforded **34** (12 mg, 63%), which was pure by NMR. ^{1}H NMR (400 MHz, DMSO-d_6) δ 11.93 (s, 1H), 10.46 (s, 1H), 7.94 (d, J = 9.0 Hz, 1H), 7.64 (m, 3H), 7.02 (d, J = 9.0 Hz, 1H), 4.31 (s, 2H), 3.71 (t, J = 5.7 Hz, 2H), 2.99 (m, 2H); ^{13}C NMR (101 MHz, DMSO-d_6) δ 190.8, 163.5, 158.1, 156.3, 153.5, 146.7, 132.3, 115.3, 114.1, 110.9, 109.3, 104.7, 43.2, 41.0, 24.2; HRMS (ESI-TOF) m/z $[M + H]^+$ calcd for $C_{14}H_{14}N_3O_4$ 288.098 43, found 288.098 81.

Allyl 7-Formyl-8-(methoxymethoxy)-5-oxo-4,5-dihydro-1*H*-chromeno[3,4-*c*]pyridine-3(2*H*)-carboxylate (35). Compound **21b** (301 mg, 914 μmol) in 5 mL of DCM at 0 °C was treated with DIEA (790 μL, 4.57 mmol) and chloromethyl methyl ether (347 μL, 4.57 mmol). The mixture was stirred for 30 h, quenched with saturated aqueous NH_4Cl, and the organic layer was washed with saturated aqueous NH_4Cl. The organic layer was dried over Na_2SO_4 and concentrated. Purification by flash column chromatography over silica gel (35%−70% EtOAc/hexanes) afforded **35** as a white solid (226 mg, 67%). ^{1}H NMR (400 MHz, $CDCl_3$) δ 10.68 (s, 1H), 7.67 (d, J = 8.9 Hz, 1H), 7.20 (d, J = 9.0 Hz, 1H), 5.95 (m, 1H), 5.35 (m, 2.5H), 5.30 (m, 0.5H), 5.24 (m, 1H), 4.64 (d, J = 5.7 Hz, 2H), 4.48 (s, 2H), 3.81 (t, J = 5.8 Hz, 2H), 3.53 (s, 3H), 2.87 (m, 2H); ^{13}C NMR (101 MHz, $CDCl_3$) δ 186.8, 160.2, 158.4, 155.0, 153.4, 145.7, 132.6, 129.4, 118.2, 117.9, 113.5, 113.3, 111.4, 94.9, 66.4, 56.8, 41.7, 39.1, 24.7; HRMS (ESI-TOF) (m/z) $[M + H]^+$ calcd for $C_{19}H_{20}NO_7$ 374.123 43, found 374.123 10.

Allyl 7-Acetyl-8-hydroxy-5-oxo-4,5-dihydro-1*H*-chromeno-[3,4-*c*]pyridine-3(2*H*)-carboxylate (36). Compound **35** (50.0 mg, 134 μmol) in 2 mL of THF at −78 °C under Ar was treated with 3 M MeMgBr in Et_2O (134 μL, 402 μmol). After 3 h at −78 °C, the reaction was carefully quenched. Then the mixture was diluted with saturated aqueous NH_4Cl, warmed to room temperature, and partitioned with EtOAc. The organic layer was dried over Na_2SO_4 and concentrated under reduced pressure to give the crude alcohol as an oil.

The above alcohol was dissolved in 3 mL of DCM and treated with Dess−Martin periodinane (123 mg, 291 μmol) and stirred at room temperature for 3 h. The reaction was quenched with 10% aqueous $Na_2S_2O_3$ and washed with brine. The organic layer was dried over Na_2SO_4, concentrated, and the residue was purified by flash column chromatography over silica gel (35−70% EtOAc/hexane) to give the intermediate ketone as a gum (34 mg, 66%, two steps). ^{1}H NMR (400 MHz, $CDCl_3$) δ 7.50 (d, J = 8.8 Hz, 1H), 7.13 (d, J = 8.9 Hz, 1H), 5.95 (m, 1H), 5.34 (m, 1H), 5.30 (m, 1H), 5.25 (m, 2.5H), 5.21 (m, 0.5H), 4.64 (d, J = 5.7 Hz, 2H), 4.45 (m, 2H), 3.80 (t, J = 5.8 Hz, 2H), 3.48 (s, 3H), 2.86 (m, 2H), 2.61 (s, 3H); ^{13}C NMR (101 MHz, $CDCl_3$) δ 199.1, 158.9, 155.6, 149.3, 145.8, 133.5, 132.7, 125.0, 120.6, 118.2, 114.0, 111.2, 108.6, 94.8, 66.7, 56.7, 42.0, 39.3, 32.7, 29.8, 24.8; HRMS (ESI-TOF) (m/z) $[M + H]^+$ calcd for $C_{20}H_{22}NO_7$ 388.139 08, found 388.139 45.

The ketone above (9.0 mg, 23 μmol) in 1.5 mL of 33% TFA/DCM solution was stirred for 1.5 h at room temperature. The mixture was concentrated under reduced pressure and the resulting residue was purified by flash column chromatography over silica gel (30% EtOAc/hexane) to afford **36** as a white foam (6.0 mg, 75%). ^{1}H NMR (400 MHz, $CDCl_3$) δ 13.54 (s, 1H), 7.63 (d, J = 8.8 Hz, 1H), 6.95 (d, J = 9.0 Hz, 1H), 5.96 (m, 1H), 5.33 (m, 2H), 5.24 (ddd, J = 10.4, 2.5, 1.2 Hz, 1H), 4.65 (dt, J = 5.7, 1.3 Hz, 2H), 4.47 (m, 2H), 3.81 (t, J = 5.8 Hz, 2H), 2.98 (s, 3H), 2.87 (m, 2H); ^{13}C NMR (101 MHz, $CDCl_3$) δ 204.4, 166.3, 158.6, 155.3, 153.8, 132.8, 130.2, 118.2, 116.6, 115.7, 111.3, 109.5, 66.7, 41.8, 39.3, 34.2, 25.1; HRMS (ESI-TOF) (m/z) $[M + H]^+$ calcd for $C_{18}H_{18}NO_6$ 344.112 86, found 344.111 16.

Allyl 7-(3-Ethoxy-3-oxoprop-1-en-1-yl)-8-hydroxy-5-oxo-4,5-dihydro-1*H*-chromeno[3,4-*c*]pyridine-3(2*H*)-carboxylate (37). Compound **35** (40.0 mg, 107 μmol) in 2 mL of DCM at room temperature was treated with triethylphosphonoacetate (48.0 mg, 139 μmol) and stirred for 20 h. The mixture was concentrated under reduced pressure. Purification by flash column chromatography over silica gel (20%−40% EtOAc/hexanes) afforded the intermediate ethyl enoate as a white solid (46 mg, 96%). ^{1}H NMR (400 MHz, $CDCl_3$) δ 8.11 (d, J = 16.4 Hz, 1H), 7.46 (m, 1H), 7.16 (d, J = 9.0 Hz, 1H), 7.05 (d, J = 16.4 Hz, 1H), 5.96 (m, 1H), 5.34 (m, 2.5H), 5.30 (m, 0.5H), 5.23 (m, 1H), 4.64 (dt, J = 5.6, 1.2 Hz, 2H), 4.46 (s, 2H), 4.28 (q, J = 7.1 Hz, 2H), 3.79 (t, J = 5.8 Hz, 2H), 3.50 (s, 3H), 2.85 (m, 2H), 1.35 (t, J = 7.1 Hz, 3H); ^{13}C NMR (101 MHz, $CDCl_3$) δ 167.8, 158.5, 151.8, 132.8, 132.7, 132.2, 132.1, 132.1, 132.0, 128.7, 128.5, 125.2, 124.4, 118.1, 113.8, 112.4, 110.9, 94.8, 66.6, 60.7, 56.8, 56.8, 42.0, 39.3, 24.9, 14.5; HRMS (ESI-TOF) (m/z) $[M + H]^+$ calcd for $C_{23}H_{26}NO_8$ 444.165 29, found 444.165 76.

The above ethyl enoate (20 mg, 45 μmol) in 2 mL of MeOH/$CHCl_3$ (3:1) at room temperature was treated with 2 mL of 4 N aqueous HCl and stirred for 18 h. The reaction was extracted with EtOAc, dried over Na_2SO_4, and concentrated under reduced pressure. Purification by flash column chromatography over silica gel (40%−70% EtOAc/hexanes) afforded **37** as a white solid (15 mg, 83%). ^{1}H NMR (400 MHz, DMSO-d_6) δ 11.57 (m, 1H), 8.01 (d, J = 16.3 Hz, 1H), 7.62 (d, J = 8.8 Hz, 1H), 6.99 (m, 2H), 5.96 (ddt, J = 17.2, 10.6, 5.3 Hz, 1H), 5.31 (m, 1H), 5.22 (m, 1H), 4.59 (dt, J = 5.3, 1.4 Hz, 2H), 4.34−4.12 (m, 4H), 3.68 (m, 2H), 2.87 (m, 2H), 1.27 (t, J = 7.1 Hz, 3H); ^{13}C NMR (101 MHz, DMSO-d_6) δ 167.0, 160.3, 158.7, 154.3, 151.7, 146.9, 133.3, 133.2, 126.7, 121.5, 117.4, 112.9, 111.3, 108.2, 65.6, 60.1, 41.3, 24.4, 14.3; HRMS (ESI-TOF) (m/z) $[M + H]^+$ calcd for $C_{21}H_{22}NO_7$ 400.139 08, found 400.139 92.

Allyl 8-Hydroxy-7-(2-(methylsulfonyl)vinyl)-5-oxo-4,5-dihydro-1*H*-chromeno[3,4-*c*]pyridine-3(2*H*)-carboxylate (38). LiCl (8.0 mg, 20 μmol) and diethyl(methylsulfonylmethyl) phosphonate (54.0 g, 236 μmol) in 2.5 mL of acetonitrile at room temperature was treated with DBU (24.0 μL, 157 μmol) and stirred for 10 min. Compound **35** (43.0 mg, 131 μmol) in 2 mL of acetonitrile was cannulated into the mixture and stirred for 2 h. The reaction was quenched with saturated aqueous NH_4Cl and extracted with EtOAc. Purification by flash column chromatography over silica gel (0−5% MeOH/$CHCl_3$) afforded the intermediate vinyl sulfone as a white solid (41 mg, 79%). ^{1}H NMR (400 MHz, $CDCl_3$) δ 8.09 (d, J = 15.8 Hz, 1H), 7.68 (d, J = 15.8 Hz, 1H), 7.56 (d, J = 8.9 Hz, 1H), 7.20 (d, J = 9.0 Hz, 1H), 5.95 (m, 1H), 5.34 (m, 2.5H), 5.30 (m, 0.5H), 5.23 (m, 1H), 4.64 (m, 2H), 4.46 (s, 2H), 3.80 (t, J = 5.8 Hz, 2H), 3.51 (s, 3H), 3.06 (s, 3H), 2.86 (m, 2H); ^{13}C NMR (101 MHz, $CDCl_3$) δ 158.8, 158.6, 155.3, 152.2, 146.1, 132.7, 131.7, 131.5, 126.8, 118.2, 113.8, 110.9, 109.9, 95.1, 66.6, 57.0, 43.3, 41.9, 39.3, 24.9; HRMS (ESI-TOF) (m/z) $[M + H]^+$ calcd for $C_{21}H_{24}NO_8S$ 450.121 72, found 450.123 90.

The above vinyl sulfone (38 mg, 84 μmol) in 2.5 mL of acetonitrile/$CHCl_3$ (2:1) was treated with 2.5 mL of 4 N aqueous HCl and stirred for 20 h at room temperature. The mixture was concentrated under reduced pressure. The resulting white solid was washed with DCM/Et_2O and the resulting solid dried to afford pure **38** (32 mg, 92%). ^{1}H NMR (400 MHz, DMSO-d_6) δ 11.78 (s, 1H), 7.87 (d, J = 15.7 Hz, 1H), 7.68 (d, J = 8.8 Hz, 2H), 7.66 (d, J = 15.7 Hz, 2H), 7.01 (d, J = 8.9 Hz, 1H), 5.97 (m, 1H), 5.31 (m, 1H), 5.21 (m, 1H), 4.59 (dt, J = 5.3, 1.5 Hz, 2H), 4.29 (s, 2H), 3.84 (s, 3H), 3.15 (s, 3H), 2.88 (s, 2H); ^{13}C NMR (101 MHz, DMSO-d_6) δ 160.5, 158.6, 154.3, 151.8, 146.9, 133.3, 130.8, 130.1, 127.6, 117.4, 112.9, 111.3, 106.5, 65.6, 42.6, 41.3, 24.2; HRMS (ESI-TOF) (m/z) $[M + H]^+$ calcd for $C_{19}H_{20}NO_7S$ 406.095 50, found 406.095 00.

3-((Allyloxy)carbonyl)-8-(methoxymethoxy)-5-oxo-2,3,4,5-tetrahydro-1*H*-chromeno[3,4-*c*]pyridine-7-carboxylic Acid (39). Compound **35** (80.0 mg, 214 μmol) and 2-methyl-2-butene (272 μL, 2.57 mmol) in 3.5 mL of *t*-BuOH/H_2O/CH_3CN (3:3:1) at 0 °C were treated with a solution of sodium chlorite (145 mg, 1.29 mmol) and sodium monophosphate (265 mg, 1.93 mmol) in water, dropwise. After 30 min the reaction was quenched with 5% aqueous $Na_2S_2O_3$. The pH of the solution was adjusted to 6, and the aqueous portion was extracted with EtOAc. The organic layer was dried over Na_2SO_4 and concentrated. Purification by flash column chromatography over silica gel (70−100% EtOAc/hexanes) afforded **39** as a thick oil (64 mg, 77%). ^{1}H NMR (400 MHz, $CDCl_3$) δ 7.57 (d, *J* = 8.2 Hz, 1H), 7.19 (d, *J* = 9.0 Hz, 1H), 6.07 (bs,12H), 5.96 (m, 1H), 5.33 (m, 2.5H), 5.24 (m, 1H), 4.65 (m, 2H), 4.48 (s, 2H), 3.82 (t, *J* = 5.7 Hz, 2H), 3.52 (s, 3H), 2.90 (m, 2H); ^{13}C NMR (101 MHz, $CDCl_3$) δ 166.5, 163.5, 162.5, 159.9, 156.9, 156.4, 155.4, 150.3, 149.7, 146.7, 132.7, 125.5, 118.3, 113.7, 113.5, 111.5, 111.1, 99.9, 95.0, 94.7, 91.8, 66.8, 56.9, 56.7, 41.9, 41.7, 39.3, 24.8; HRMS (ESI-TOF) (*m*/*z*) [M + H]$^+$ calcd for $C_{19}H_{20}NO_8$ 390.118 35, found 390.117 50.

3-((Allyloxy)carbonyl)-8-hydroxy-5-oxo-2,3,4,5-tetrahydro-1*H*-chromeno[3,4-*c*]pyridine-7-carboxylic Acid (40). Compound **39** (32 mg, 82 μmol) in 1 mL of MeOH was treated with 2 mL of 4 N aqueous HCl and stirred for 20 h at room temperature. The mixture was concentrated under reduced pressure. Purification by semi-preparative RP-HPLC (C_{18} column, 0−70% MeCN/H_2O gradient over 20 min) and subsequent lyophilization afforded compound **40** as a white solid (12 mg, 56%). ^{1}H NMR (400 MHz, CD_3CN) δ 12.39−11.57 (m, 1H), 7.75 (d, *J* = 9.0 Hz, 0.7H), 7.69 (rotamer: d, *J* = 8.9 Hz, 0.3H), 6.95 (dd, *J* = 9.0, 1.0 Hz, 0.7H), 6.85 (rotamer: d, *J* = 8.9 Hz, 0.3H), 5.99 (m, 1H), 5.32 (m, 1H), 5.21 (m, 1H), 4.61 (m, 2H), 4.31 (s, 2H), 3.73 (m, 2H), 2.86 (m, 2H); ^{13}C NMR (101 MHz, CD3CN) δ 171.4, 165.9, 159.7, 153.7, 148.9, 147.7, 134.3, 131.4, 130.4, 117.6, 116.1, 115.0, 112.9, 102.5, 66.8, 42.4, 42.3, 25.6; HRMS (ESI-TOF) (*m*/*z*) [M + H]$^+$ calcd for $C_{17}H_{16}NO_7$ 346.092 13, found 346.091 98.

3-Allyl 7-Methyl-8-hydroxy-5-oxo-4,5-dihydro-1*H*-chromeno[3,4-*c*]pyridine-3,7(2*H*)-dicarboxylate (41). Compound **39** (20 mg, 51 μmol) in 2 mL of acetone at room temperature was treated with potassium carbonate (10 mg, 77 μmol) and methyl iodide (5.0 μL, 77 μmol) and stirred for 24 h. The mixture was diluted with EtOAc, washed with brine, and dried over Na_2SO_4. Purification by flash column chromatography over silica gel (50−70% EtOAc/hexanes) afforded the intermediate methyl ester as a thick oil (10 mg, 48%). ^{1}H NMR (400 MHz, $CDCl_3$) δ 7.51 (d, *J* = 8.2 Hz, 1H), 7.13 (d, *J* = 9.0 Hz, 1H), 5.94 (m, 1H), 5.37−5.18 (m, 4H), 4.63 (m, 2H), 4.44 (s, 2H), 3.98 (s, 3H), 3.78 (t, *J* = 5.8 Hz, 2H), 3.48 (m, 3H), 2.85 (m, 2H); ^{13}C NMR (101 MHz, $CDCl_3$) δ 164.4, 163.5, 158.8, 156.3, 150.1, 145.6, 132.8, 125.6, 125.4, 118.2, 113.9, 113.4, 111.2, 94.8, 91.9, 66.7, 56.7, 53.2, 42.2, 39.3, 24.8; HRMS (ESI-TOF) (*m*/*z*) [M + H]$^+$ calcd for $C_{20}H_{22}NO_8$ 404.133 99, found 404.134 65.

The above ester (10 mg, 25 μmol) was treated with 1.5 mL of 33% TFA/DCM at room temperature and stirred for 1 h. The excess TFA was removed under reduced pressure to afford **41** as a semisolid (8.0 mg, 90%). ^{1}H NMR (400 MHz, $CDCl_3$) δ 11.96 (bs, 1H), 7.63 (d, *J* = 8.5 Hz, 1H), 7.01 (d, 8.9 Hz, 1H), 5.95 (m, 1H), 5.33 (m, 1H), 5.25 (m, 1H), 4.66 (m, 2H), 4.49 (s, 2H), 4.08 (s, 3H), 3.80 (m, 2H), 2.88 (m, 2H); ^{13}C NMR (101 MHz, $CDCl_3$) δ 170.4, 165.3, 152.8, 152.6, 146.8, 132.5, 129.5, 118.5, 115.1, 111.9, 102.2, 101.0, 67.0, 53.5, 41.8, 39.5, 25.0; HRMS (ESI-TOF) (*m*/*z*) [M + H]$^+$ calcd for $C_{18}H_{18}NO_7$ 360.107 78, found 360.107 59.

Allyl 8-Hydroxy-7-(methoxy(methyl)carbamoyl)-5-oxo-4,5-dihydro-1*H*-chromeno[3,4-*c*]pyridine-3(2*H*)-carboxylate (42). Compound **39** (91.0 mg, 276 μmol) and 2-methyl-2-butene (350 μL, 3.31 mmol) in 3.5 mL of CH_3CN/H_2O (1:1) at 0 °C was treated with a solution of sodium chlorite (187 mg, 1.66 mmol) and sodium monophosphate (343 mg, 2.48 mmol) in water, dropwise. After the mixture was stirred for 1 h, the reaction was quenched with 5% aqueous $Na_2S_2O_3$ solution in water. The pH of the solution was adjusted to 6 and the aqueous portion extracted with EtOAc. The organic layer was dried over Na_2SO_4 and concentrated under reduced pressure.

The resulting thick oil was dissolved in 4 mL of DCM and treated with 4-*N*-methylmorpholine (60 μL, 540 μmol), *N*,*O*-dimethylhydroxylamine hydrochloride (27 mg, 280 μmol), and EDC (53 mg, 280 μmol). The mixture was stirred for 20 h at room temperature, diluted with DCM, and washed with 1 M aqueous HCl. The organic layer was dried over Na_2SO_4 and concentrated under reduced pressure. Purification by flash column chromatography over silica gel (3−6% MeOH/$CHCl_3$) gave the intermediate Weinreb amide as a gum (61 mg, 51%, two steps). ^{1}H NMR (400 MHz, $CDCl_3$) δ 7.50 (d, *J* = 8.6 Hz, 1H), 7.14 (t, *J* = 7.8 Hz, 1H), 5.94 (m, 1H), 5.28 (m, 4H), 4.63 (d, *J* = 5.6 Hz, 2H), 4.42 (m, 2H), 3.96 (s, 0.5H), 3.73 (m, 2H), 3.48 (m, 5.5H), 3.43 (m, 2.5H), 3.14 (s, 0.5H), 2.87 (s, 2H); ^{13}C NMR (101 MHz, $CDCl_3$) δ 164.3, 159.1, 155.8, 155.3, 149.5, 145.8, 132.8, 125.4, 124.7, 118.2, 115.0, 113.8, 111.1, 94.7, 66.6, 61.8, 61.2, 56.7, 42.1, 39.3, 35.8, 32.4, 24.8; HRMS (ESI-TOF) (*m*/*z*) [M + H]$^+$ calcd for $C_{21}H_{25}N_2O_8$ 433.160 54, found 433.158 86.

The above amide (15 mg, 35 μmol) was treated with 1.5 mL of 33% TFA/DCM at room temperature and stirred for 2 h. The excess TFA was removed under reduced pressure to afford pure **42** as a semisolid (13 mg, 96%). ^{1}H NMR (400 MHz, $CDCl_3$) δ 7.49 (bs, 1H), 6.96 (d, *J* = 7.2 Hz, 1H), 6.88−6.35 (bs 1H), 5.94 (m, 1H), 5.33 (m, 1H), 5.24 (m, 1H), 4.65 (m, 2H), 4.45 (m, 2H), 3.80 (m, 2H), 3.75−3.50 (bs, 3H), 3.39 (s, 3H), 2.87 (m, 2H); ^{13}C NMR (101 MHz, $CDCl_3$) δ 159.2, 158.9, 155.4, 150.0, 146.6, 132.6, 126.4, 118.3, 116.9, 114.2, 112.0, 108.8, 76.6, 76.5, 66.8, 61.8, 41.9, 39.4, 24.9; HRMS (ESI-TOF) (*m*/*z*) [M + H]$^+$ calcd for $C_{19}H_{21}N_2O_7$ 389.134 33, found 389.133 65.

Recombinant Human IRE-1 Expression and Purification. Expression of 59.2 kDa polyhistidine-tagged puritin-hIRE-1 fusion protein was carried out in SF21 cells using the Bac to Bac expression system (Invitrogen) according to manufacturer's specifications. An 8×-His-puritin sequence was fused to the N-terminal end of the cytoplasmic kinase/RNase domain of human IRE-1 (aa 547−977) in the pFastbacDual-PBL expression vector and included a PreScission protease cleavage site in the linker. Frozen insect cell paste (1 g) was suspended in 8 mL of lysis buffer (50 mM Tris-HCl, pH 8.0, 300 mM NaCl, 5 mM βME, 10 mM imidazole) containing one protease inhibitor tablet and lysed using sonication. After removal of the cell debris via centrifugation, the supernatant was applied to a Ni(NTA) column (5 mL). After the untagged protein was washed by flushing with 10 column volumes of lysis buffer, the target protein was eluted using a linear imidazole gradient (15 column volumes, 10−300 mM). Fractions were analyzed via SDS−PAGE. Pooled protein-containing fractions were concentrated and rebuffered into 50 mM Tris, pH 8.0, 150 mM NaCl, 1 mM DTT via ultrafiltration. Typically, 1 L of insect cell culture yielded 3 mg of recombinant 8×-His-puritin-hIRE-1 following Ni(NTA) column purification.

In Vitro IRE-1 RNase FRET-Suppression Assay. The endoribonuclease activity of recombinant hIRE-1 was assayed by incubation of 50 μL of 10 nM hIRE-1 and 50 μL of various concentrations (0.01−1 μM) of fluorescently tagged XBP-1 RNA stem loop (5′-Cy5-CAGUCCGCAGCACUG-BHQ-3′, obtained from Sigma-Aldrich Co.) in assay buffer (20 mM HEPES, pH 7.5, 50 mM KOAc, 0.5 mM $MgCl_2$, 3 mM DTT, 0.4% PEG, and 5% DMSO) for up to 2 h at room temperature in a black 96-well plate. Fluorescence was read at various time points using a Biotek Synergy H1 plate reader with excitation and emission at 620 and 680 nm, respectively. The K_m of purified recombinant hIRE-1 was determined to be 45 nM using the Michaelis−Menten kinetic model. Inhibition of RNA cleavage by small molecules was determined by preincubation of 40 μL of 15 nM hIRE-1 with various concentrations of compounds (40 μL) in assay buffer for 30 min at room temperature. A 150 nM solution of fluorescent XBP-1 RNA (40 μL) was then added to each well and the reaction allowed to proceed for 2 h before reading fluorescence as described above. Final concentrations of hIRE-1 and XBP-1 RNA were 5 and 50 nM, respectively. All fluorescence readings were corrected using background values from wells containing only 120 μL of 50 nM XBP-1 RNA. Dose−response experiments were carried out a minimum of 4 times on different days and IC_{50} values calculated from the mean inhibition value at each concentration.

dx.doi.org/10.1021/jm5002452 | J. Med. Chem. 2014, 57, 4289−4301

Antibodies and Reagents. Antibodies against IRE-1 (Cell Signaling), PARP (Cell Signaling), XBP-1s (Santa Cruz), p97 (Fitzgerald), and actin (Sigma), were obtained commercially.

Cell Culture. Primary B cells were purified from wild-type mouse spleens by negative selection using anti-CD43 magnetic beads (Miltenyi Biotech). These cells as well as the human mantle cell lymphoma (MCL) cell lines Mino and Jeko were cultured in RPMI 1640 medium (Gibco) supplemented with 10% heat-inactivated fetal bovine serum (FBS), 2 mM L-glutamine, 100 U/mL penicillin G sodium, 100 μg/mL streptomycin sulfate, 1 mM sodium pyruvate, 0.1 mM nonessential amino acids, and 0.1 mM β-mercaptoethanol (β-ME).

Protein Isolation and Immunoblotting. Cells were lysed using RIPA buffer (10 mM Tris-HCl, pH 7.4; 150 mM NaCl; 1% NP-40; 0.5% sodium deoxycholate; 0.1% SDS; 1 mM EDTA) supplemented with protease inhibitors (Roche). Protein concentrations were determined by BCA assays (Pierce). Samples were boiled in SDS–PAGE sample buffer (62.5 mM Tris-HCl, pH 6.8; 2% SDS; 10% glycerol; 0.1% bromophenol blue) with β-ME and analyzed by SDS–PAGE. Proteins were transferred to nitrocellulose membranes, blocked in 5% nonfat milk (wt/vol in PBS), and immunoblotted with indicated primary antibodies and appropriate horseradish peroxidase-conjugated secondary antibodies. Immunoblots were developed using Western Lighting chemiluminescence reagent (PerkinElmer).

Cell Proliferation XTT Assays. Appropriate numbers of cells were suspended in phenol red-free culture medium, seeded in 96-well cell culture plates, and treated with indicated IRE-1 inhibitors. After 48 h, cells were spun down and proliferation was assessed by XTT assays (Roche) according to the manufacturer's instructions. Briefly, 50 μL of XTT labeling reagent, 1 μL of electron-coupling reagent, and 100 μL of phenol red-free culture medium were combined and applied to each well of the 96-well plates. Cells were then incubated for 4 h in a CO_2 incubator to allow for the yellow tetrazolium salt XTT to be cleaved by mitochondrial dehydrogenases of metabolic active cells to form the orange formazan dye, which can be quantified at 492 nm using a BioTek Synergy H1 microplate reader.

■ ASSOCIATED CONTENT

Supporting Information

^{1}H NMR spectra for assayed inhibitors, kinetic RNase activity data for recombinant IRE-1, FRET-suppression assay dose–response curves for all active inhibitors, stability data for compound **24**, and XTT assay with **30** in the presence of mouse B cells. This material is available free of charge via the Internet at http://pubs.acs.org.

■ AUTHOR INFORMATION

Corresponding Authors

*J.R.D.V.: phone, 813-745-6142; fax, (813) 745-6817; e-mail, juan.delvalle@moffitt.org.

*C.-C.A.H.: phone, 813-745-4167; e-mail, chih-chi.hu@moffitt.org.

Notes

The authors declare no competing financial interest.

■ ACKNOWLEDGMENTS

This work was supported by the National Institutes of Health (Grant R01CA163910), the American Cancer Society (Grants IRG9309214 and IRG9303216), a Moffitt Team Science award, and the Miles for Moffitt Foundation.

■ ABBREVIATIONS USED

XBP-1s, X-box binding protein 1 spliced form; FRET, fluorescence resonance energy transfer; HMBC, heteronuclear multiple bond correlation; CI, confidence interval

■ REFERENCES

(1) Rutkowski, D. T.; Hegde, R. S. Regulation of basal cellular physiology by the homeostatic unfolded protein response. *J. Cell Biol.* **2010**, *189*, 783–794.

(2) Walter, P.; Ron, D. The unfolded protein response: from stress pathway to homeostatic regulation. *Science* **2011**, *334*, 1081–1086.

(3) Shen, X.; Ellis, R. E.; Lee, K.; Liu, C. Y.; Yang, K.; Solomon, A.; Yoshida, H.; Morimoto, R.; Kurnit, D. M.; Mori, K.; Kaufman, R. J. Complementary signaling pathways regulate the unfolded protein response and are required for *C. elegans* development. *Cell* **2001**, *107*, 893–903.

(4) Yoshida, H.; Matsui, T.; Yamamoto, A.; Okada, T.; Mori, K. XBP1 mRNA is induced by ATF6 and spliced by IRE1 in response to ER stress to produce a highly active transcription factor. *Cell* **2001**, *107*, 881–891.

(5) Calfon, M.; Zeng, H.; Urano, F.; Till, J. H.; Hubbard, S. R.; Harding, H. P.; Clark, S. G.; Ron, D. IRE1 couples endoplasmic reticulum load to secretory capacity by processing the XBP-1 mRNA. *Nature* **2002**, *415*, 92–96.

(6) Wang, S.; Kaufman, R. J. The impact of the unfolded protein response on human disease. *J. Cell Biol.* **2012**, *197*, 857–867.

(7) Luo, J.; Solimini, N. L.; Elledge, S. J. Principles of cancer therapy: oncogene and non-oncogene addiction. *Cell* **2009**, *136*, 823–837.

(8) Feldman, D. E.; Chauhan, V.; Koong, A. C. The unfolded protein response: a novel component of the hypoxic stress response in tumors. *Mol. Cancer Res.* **2005**, *3*, 597–605.

(9) Romero-Ramirez, L.; Cao, H.; Nelson, D.; Hammond, E.; Lee, A. H.; Yoshida, H.; Mori, K.; Glimcher, L. H.; Denko, N. C.; Giaccia, A. J.; Le, Q. T.; Koong, A. C. XBP1 is essential for survival under hypoxic conditions and is required for tumor growth. *Cancer Res.* **2004**, *64*, 5943–5947.

(10) Hetz, C.; Chevet, E.; Harding, H. P. Targeting the unfolded protein response in disease. *Nat. Rev. Drug Discovery* **2013**, *12*, 703–719.

(11) Yu, C. Y.; Hsu, Y. W.; Liao, C. L.; Lin, Y. L. Flavivirus infection activates the XBP1 pathway of the unfolded protein response to cope with endoplasmic reticulum stress. *J. Virol.* **2006**, *80*, 11868–11880.

(12) Martinon, F.; Chen, X.; Lee, A. H.; Glimcher, L. H. TLR activation of the transcription factor XBP1 regulates innate immune responses in macrophages. *Nat. Immunol.* **2010**, *11*, 411–418.

(13) Todd, D. J.; McHeyzer-Williams, L. J.; Kowal, C.; Lee, A. H.; Volpe, B. T.; Diamond, B.; McHeyzer-Williams, M. G.; Glimcher, L. H. XBP1 governs late events in plasma cell differentiation and is not required for antigen-specific memory B cell development. *J. Exp. Med.* **2009**, *206*, 2151–2159.

(14) Papandreou, I.; Denko, N. C.; Olson, M.; Van Melckebeke, H.; Lust, S.; Tam, A.; Solow-Cordero, D. E.; Bouley, D. M.; Offner, F.; Niwa, M.; Koong, A. C. Identification of an Ire1alpha endonuclease specific inhibitor with cytotoxic activity against human multiple myeloma. *Blood* **2011**, *117*, 1311–1314.

(15) Cross, B. C.; Bond, P. J.; Sadowski, P. G.; Jha, B. K.; Zak, J.; Goodman, J. M.; Silverman, R. H.; Neubert, T. A.; Baxendale, I. R.; Ron, D.; Harding, H. P. The molecular basis for selective inhibition of unconventional mRNA splicing by an IRE1-binding small molecule. *Proc. Nat. Acad. Sci. U.S.A* **2012**, *109*, E869–E878.

(16) Mimura, N.; Fulciniti, M.; Gorgun, G.; Tai, Y. T.; Cirstea, D.; Santo, L.; Hu, Y.; Fabre, C.; Minami, J.; Ohguchi, H.; Kiziltepe, T.; Ikeda, H.; Kawano, Y.; French, M.; Blumenthal, M.; Tam, V.; Kertesz, N. L.; Malyankar, U. M.; Hokenson, M.; Pham, T.; Zeng, Q.; Patterson, J. B.; Richardson, P. G.; Munshi, N. C.; Anderson, K. C. Blockade of XBP1 splicing by inhibition of IRE1alpha is a promising therapeutic option in multiple myeloma. *Blood* **2012**, *119*, 5772–5781.

(17) Volkmann, K.; Lucas, J. L.; Vuga, D.; Wang, X.; Brumm, D.; Stiles, C.; Kriebel, D.; Der-Sarkissian, A.; Krishnan, K.; Schweitzer, C.; Liu, Z.; Malyankar, U. M.; Chiovitti, D.; Canny, M.; Durocher, D.; Sicheri, F.; Patterson, J. B. Potent and selective inhibitors of the inositol-requiring enzyme 1 endoribonuclease. *J. Biol. Chem.* **2011**, *286*, 12743–12755.

(18) Ri, M.; Tashiro, E.; Oikawa, D.; Shinjo, S.; Tokuda, M.; Yokouchi, Y.; Narita, T.; Masaki, A.; Ito, A.; Ding, J.; Kusumoto, S.; Ishida, T.; Komatsu, H.; Shiotsu, Y.; Ueda, R.; Iwawaki, T.; Imoto, M.; Iida, S. Identification of toyocamycin, an agent cytotoxic for multiple myeloma cells, as a potent inhibitor of ER stress-induced XBP1 mRNA splicing. *Blood Cancer J.* **2012**, *2*, e79.
(19) Wang, L.; Perera, B. G.; Hari, S. B.; Bhhatarai, B.; Backes, B. J.; Seeliger, M. A.; Schurer, S. C.; Oakes, S. A.; Papa, F. R.; Maly, D. J. Divergent allosteric control of the IRE1alpha endoribonuclease using kinase inhibitors. *Nat. Chem. Biol.* **2012**, *8*, 982−989.
(20) Singh, J.; Petter, R. C.; Baillie, T. A.; Whitty, A. The resurgence of covalent drugs. *Nat. Rev. Drug Discovery* **2011**, *10*, 307−317.
(21) Tomasio, S. M.; Harding, H. P.; Ron, D.; Cross, B. C.; Bond, P. J. Selective inhibition of the unfolded protein response: targeting catalytic sites for Schiff base modification. *Mol. BioSyst.* **2013**, *9*, 2408−2416.
(22) Kriss, C. L.; Pinilla-Ibarz, J. A.; Mailloux, A. W.; Powers, J. J.; Tang, C. H.; Kang, C. W.; Zanesi, N.; Epling-Burnette, P. K.; Sotomayor, E. M.; Croce, C. M.; Del Valle, J. R.; Hu, C. C. Overexpression of TCL1 activates the endoplasmic reticulum stress response: a novel mechanism of leukemic progression in mice. *Blood* **2012**, *120*, 1027−1038.
(23) Ogata, Y.; Kawasaki, A.; Sugiura, F. Kinetics and mechanism of the Duff reaction. *Tetrahedron* **1968**, *24*, 5001−5010.
(24) Blazzevic, N.; Kolbah, D.; Belin, B.; Sunjic, V.; Kajfez, F. Hexamethylenetetramine, a versatile reagent in organic synthesis. *Synthesis* **1979**, 161−176.
(25) Hu, C. C.; Dougan, S. K.; McGehee, A. M.; Love, J. C.; Ploegh, H. L. XBP-1 regulates signal transduction, transcription factors and bone marrow colonization in B cells. *EMBO J.* **2009**, *28*, 1624−1636.
(26) Mimura, N.; Fulciniti, M.; Gorgun, G.; Tai, Y.-T.; Cirstea, D.; Santo, L.; Hu, Y.; Fabre, C.; Minami, J.; Ohguchi, H.; Kiziltepe, T.; Ikeda, H.; Kawano, Y.; French, M.; Blumenthal, M.; Tam, V.; Kertesz, N. L.; Malyankar, U. M.; Hokenson, M.; Pham, T.; Zeng, Q.; Patterson, J. B.; Richardson, P. G.; Munshi, N. C.; Anderson, K. C. Blockade of XBP1 splicing by inhibition of IRE1α is a promising therapeutic option in multiple myeloma. *Blood* **2012**, *119*, 5772−5781.

■ NOTE ADDED AFTER ASAP PUBLICATION

Due to a production error, the IC_{50} curve and Western Blot gel in the abstract graphic were omitted from the version published on May 2, 2014. The revised version was reposted on May 2, 2014.